nature portfolio

Peer Review File

Single-cell multiomics uncovers an endothelial mechanosensitive PIEZO1-IL-33 axis driving pulmonary fibrosis

Corresponding Author: Professor Shanze Chen

This file contains all reviewer reports in order by version, followed by all author rebuttals in order by version.

Version 0:

Reviewer comments:

Reviewer #1

(Remarks to the Author)
This is an original manuscript from Zhang and colleagues exploring the role of PIEZO1 on endothelial cells in mouse models of pulmonary fibrosis. Reporting a small snRNA-seq dataset and analyzing other public resources, they suggest that there are increased endothelial cells in IPF lungs with evidence of mechanical stress, and in several preclinical fibrosis models, suggest that endothelial-cell Piezo1 is a potential driver of this. Several conditional deletion models and ex-vivo studies suggest that endothelial cell specific Piezo1 activation promotes fibrosis in an IL33 dependent manner. There has been limited study of the endothelium in pulmonary fibrosis pathogenesis and these studies offer potential new insights. There are a number of substantive analytical issues the authors need to address.

Major comments:
1) Figure 1: The assertion that there are increased endothelial cells in IPF lungs is at odds with considerable prior work and assessment of histopathology. These results are likely an artifact of small numbers, sampling methods, and statistical treatment. The resolution of annotation of this new snRNA-seq dataset is very low, and could be substantially improved using any of a number of public datasets as a reference. This influences much of the downstream analysis. First, snRNA-seq of IPF and control lungs – lumping all endothelial cells for analysis of cell composition is not really meaningful (capillaries, venules, arterioles, etc are anatomically and functionally distinct). Second, assessment of cell composition from n of 3 samples is not robust (particularly as the authors could have assessed this from the meta-analyzed dataset presented later in the figure). Third, since composition is a “zero-sum” scenario, Bayesian methods (i.e. propeller or others) are more appropriate.

2) Figure 1: FVC-based classification as utilized by the authors reflects disease stage (not progression). The authors are not reporting an FVC rate of change (which would be an indicator of progression rate), but are reporting FVC which at one point in time is a measure of disease severity. Those with an FVC <50 do not necessarily have more rapidly progressive disease, they simply have had disease longer than those with and FVC >50%. This should be clarified in the text and figure legend.

3) Figure 1F: Numerous manuscripts have described COL15A1+/PLVAP+ “systemic-venous-like” endothelial cells as markedly more abundant in IPF lungs yet are not described in this figure – are these being misclassified as “capillary cells”?

4) Lacking code availability or reporting of the genes which were used in the “mechanical stress” gene score, it is difficult to assess the robustness and reliability of this finding.

5) Figures 2 and 3 – similar to the above comment, lumping all endothelial cells into a single population risks conflating changes in relative abundance of certain anatomically distinct populations with changes in chromatin accessibility and gene expression within a population. There are well-established marker genes that can discriminate endothelial cell subtypes into aCap, gCap, venule, arteriole and lymphatic populations at minimum to report these data.

6) Figure 3 – PIEZO2 is essentially not expressed in the vascular endothelium, so it is unclear what a ratio of Piezo1+/Piezo2+ cells would mean

7) Figure 4: Fibrosis assessments are reported as an “Inflammation Score” and “Relative Collagen Content” but no methods for these assessments are reported. Standard measures of fibrosis assessment (quantification of fibrotic area or Ashcroft score) in addition to hydroxyproline should be reported.

8) No quantitative measurements of fibrosis are reported for the GsMTx4 or Yoda1 treatment studies in Figure 4I – any assertions of effects on fibrosis need to be supported by appropriate quantitative measures and statistical treatment.

9) Figure 5 – cell communication analyses are really only informative at cell-type resolution – the finding that Piezo1 is correlated with Ackr1 (a specific marker of veins/venules) suggests that these findings overall reflect compositional differences within the endothelial cell population (rather than changes in cell-type specific expression related to Piezo1 expression).

10) Figure 5J – the image quality is very low and not interpretable

11) Figure 6 – same comment as #7 – results regarding fibrosis need to be supported by standard, validated, methods for quantification of fibrosis.

Minor comments:
1) Figure 2E: ILC’s should not express Cd3e, the authors should check this annotation and/or evaluate ambient RNA contamination
2) Results for Figure 3: “To investigate the subcellular distribution of PIEZOs in ECs, we analyzed human lung ECs using scRNA-seq bubble plots” – semanic point, but “bubble plots” are a visualization tool, not an analysis, and they report cellular (not “subcellular”) expression – the text for this sentence should be edited to clarify this

Reviewer #2

(Remarks to the Author)
This paper by Zhang, Zhang, Gui, Xia et al., looks at the role of endothelial PIEZO1 channels in the development of pulmonary fibrosis in two animal models. Using a Cre-lox strategy to specifically delete Piezo1 from endothelial cells they link PIEZO1 to the fibrotic cascade and attempt to link these effects to IL-33. Despite the raft of bioinformatics approaches the attempts to link this directly to mechanical stress are poorly fleshed out, for example a reader is still left with the question of exactly what cue is stimulating ECs in response to bleomycin or SiO2 to drive pulmonary fibrosis? This seems like a key question that the authors do a poor job of discussing. In addition, the use of PIEZO1 pharmacology is also rudimentary and there is no discussion of the off-target effects of GsMTx-4 or the fact that Yoda-1 drives cellular Ca2+ signalling that is spatio-temporally different from the mechanical activation of PIEZO1 (this is especially important for the in vitro experiments). Despite this, the data from KO mice and human datasets is compelling that PIEZO1 in ECs plays a role in the development of pulmonary fibrosis. The effects on IL-33 are strong and PIEZO1-dependent providing high level confidence that a PIEZO1-IL-33 pathway is at play in these disease models. I have a number of points below that require addressing prior to publication especially related to the in vitro experiments in HUVEC.
Just a general point the lack of line numbering makes reviewing arduous!
1) Why is the control haplo-insufficient – what’s its genotype? I assume this is a typo.
2) PIEZO1 vs Piezo1 needs uniformity.
3) Figure 4B comes from isolated ECs or whole tissue? If whole tissue how is the reduction so profound given all other cell types express PIEZO1. Figure 4I lacks quantification shown in Figure 4D.
4) For Figure 7 a calpain assay would be much better than mRNA levels. It’s not clear why Yoda1 would increase the mRNA levels of calpain2(or STAT3 – STAT3 also doesn’t come up earlier in the omics sections). The pathway should be dictated by Ca2+ induced activation of calpain – in this scenario as a homeostatic mechanism one might expect a reduction in calpain levels under a sustained mechanical cue not an increase. Using Yoda1 as a surrogate for mechanical stress is fraught with danger as it induces spatio-temporal Ca2+ signalling that is wholly different to mechanically induced PIEZO1 signalling. In a mechanical response PIEZO1 signalling is localized to certain regions like focal adhesions (Chen et al., 2018 Neuron; Yao et al., 2022 Science advances) and is transient. This is very different from when yoda1 is added – which causes a tonic sustained elevation in intracellular Ca2+. It is necessary to show the same pathway in response to a relevant mechanical cue. The reason for this is that if you use Yoda1 in an in vitro system you can end up suggesting a pathway like seen in cardiac PIEZOs (Zhang et al., 2021 Hypertension) that ends up being incorrect (Yu et al., 2022 Nature Cardiovascular Research). At least a mechanical cue should be used to validate these findings (stretch, stiffness, shear stress etc). This links back to the major question of what cue is driving this signalling in these disease models!!
5) There's also no data that IL-33 is actually released. An ELISA showing PIEZO1-mediated release of IL-33 is really essential as generally speaking the paper is too reliant on mRNA levels to suggest mechansim.

Reviewer #3

(Remarks to the Author)
Zhang et al. present a study “Single-cell multiomics reveals endothelial mechanosensitive PIEZO1 coupling IL33 regulates the development of pulmonary fibrosis” that uncovers a molecular mechanism of pulmonary fibrosis (PF). PF is a lethal disease with limited treatment options. By analyzing sc/nRNA-seq and scATAC-seq data from human specimens and two mouse models (silica and Bleomycin induced) the study authors identify upregulation of genes linked to mechanosensation in endothelial cells. They identify PIEZO1 as top candidate and validate its role using genetic deletion in a mouse model and small molecule inhibition or activation. They could show that blocking or deleting PIEZO1 decreases fibrosis and

activation resulted in increased fibrosis. Finally, they show that PIEZO1 couples to IL33 and activates a CAPN2-STAT3 signalling cascade.
This is an exciting, comprehensive and well executed study covering hypothesis generating single cell data and follow-up analysis using genetic mouse models and small molecules to validate predictions for the role of PIEZO1 and related signaling in PF.

I have a few comments that would need to be addressed:

1) According to Table S1 and S2 only 5 donors were profiled? Where does the sixth datapoint in the figures come from? Please clarify.
2) What genes are in the MS Score? How was the statistic calculated in 1N, 2H, 2J. Per individual or per cell?
3) MS Score analysis shows an increase in PF in the silica model (2H, 2J), but in the Bleomycine model mostly Piezo1/2 are robustly regulated (3K). How can this be explained?
4) The scATAC-seq data lacks analytical details, e.g. how were cells filtered? How was peak calling performed? How was transcription factor motif enrichment performed? How was batch correction performed and doublets removed (also for scRNA data)?
5) Fig 2L “different thematic patterns of ECs” -> TF motif enrichment analysis? How was this analysis performed, which tool was used? Is this analysis performed on all ECs or differential accessible sites (same for Bleomyin analysis)? What about all the other motifs except STAT motif that were identified from the scATAC analysis?
6) 3G what exactly is displayed: Figure panel states motif and legend states an AUC score of mechanical stress genes.
7) 7J there is no binding of STAT3 at the promoter region of IL33 on the tracks visible. The signal of STAT3 at most sites is lower after YODA1 treatment despite the model would suggest otherwise. Do all peaks have a STAT3 binding site?
8) 7H why top 100 and top 10 TFs (text states top 7)? How was this determined? What are the “top 10 transcription factors”? How was it concluded that it must be STAT3 and not for example STAT1 which was labeled as enriched motif in 2L and S5L. Motif analysis usually cannot pin down the exact factor so both could be options.

Minor:
1) From the writing it is unclear if the processing and annotation of scATAC-seq of Silica and BLM datasets (one mentions annotation based on prediction from scRNA and the latter looks at promoter accessibility). Please clarify.
2) S4 panel legend F and G is switched. S5 description for panel I is incorrect.

Version 1:

Reviewer comments:

Reviewer #1

(Remarks to the Author)
The authors have made extensive revisions to the manuscript in response to critiques from the reviewers. While several responses have addressed my prior comments and have improved the manuscript significantly, there are a number of issues that have not be adequately resolved and in places the revised results raise points that should be addressed.
1) The authors have removed textual assertions of increased endothelial cells in IPF lungs, although Figure 1D legend continues to state this. In the response letter, they support this assertion by citing three small scRNA-seq datasets. Because of issues related to cellular/nuclear disaggregation (particularly from fibrotic lungs), the assertion that sc/snRNA-seq more precisely quantifies cellular composition compared to histologic/tissue-based methods is not accurate. Specifically, relatively increased proportions of endothelial cells can be recovered when there is poor liberation or viability of alveolar epithelial cells and fibroblasts.
a. The plot from the Caporarello Nature Communications manuscript is plotting subpopulations of endothelial cells using total endothelial cells as the denominator – this is not quantifying endothelial cells in relation to total cells. Further, the cited reference for the primary date underlying that plot appears potentially incorrect – the reference refers to GSE136831 which included 32 IPF and 27 control lungs, yet only 3 dots per group are shown in this plot. Altogether, these results simply do not support the authors assertion that endothelial cells are increased in IPF lungs.
b. The other referenced examples presented in the response letter (none of which report statistical differences in endothelial cells using appropriate methods including multiple testing correction), also suffer from the same “zero-sum” issue previously raised – if one population is reduced in scRNA-seq (for example, AT1 and AT2 cells), one must recover a larger proportion of other cell populations, even if absolute numbers are decreased – this is simply not a reliable method for compositional analyses.
c. Further, the largest IPF/ILD scRNA-seq datasets (GSE136831, GSE227136) show the opposite finding (while there are increased COL15A1+ systemic-venous type endothelial cells, dramatic reductions in capillary endothelial cells result in an overall decrease). In addition, three recent tissue-based spatial transcriptomic studies (PMID 38951642, 39121212, 39901013) also show, if anything, reduced endothelial cells – these methods, which are more accurate for compositional assessment than any disaggregation-based scRNA-seq method, should be considered much closer to a “gold standard.”
d. The overall assertion of increased endothelial cells in IPF lungs is not ultimately very relevant to the authors proposed (and better supported) mechanistic studies, so I would recommend the compositional analyses and claims related to them be removed.
2) The revised cell annotation appears much improved and more useful for readers to compare across publications and interpret these results
3) The increased number of samples (now 4-5 per group) represents an improvement, though this is still a small dataset compared to the 100+ public IPF samples available

4) The revised language clarifying that single-timepoint FVC reflects severity, not progression rate, is acceptable
5) It is appreciated that the authors report the genes used for the “mechanical stress” score, but shouldn’t the same set of genes be used for each of the analyses? It isn’t clear why a different set of genes was used for human vs. house and was not consistent within human or within mouse experiments.
6) The revised fibrosis measures are improved, although in some experiments (Figure 4H-K, non-bleomycin treated controls are not reported.
7) Revised Figure 1G: this still appears to be plotting differentially expressed genes across the entire endothelial cell group, which will reflect compositional differences. Subject-level, cell-type specific pseudobulk differential expression would be the rigorous and robust means of testing for differentially expressed genes among IPF subjects.
8) In line with comments from Reviewer 3, the Yoda-studies lack specificity; to have high confidence that these studies are mediating their effects through endothelial Piezo 1, it would be necessary to test whether Yoda-treatment of endothelial Piezo1-deficient animals did or did not augment fibrosis.
9) The revised calpain studies add some strength to the overall body of evidence
10) In several panels where there are many groups in bar-plots(for example, figures 4 and 6), the statistical methods need to be included in the figure legends - it is difficult to assess these lacking details as to multiple testing adjustments, etc.

Minor comments:
1) For many figure legends, there is a space missing between Figure and the number.
2) In numerous places, the revised figure legends are interpretative of the results rather than descriptive of the study – the legends should describe the experiment, and any interpretation belongs in the main text (1D, 1H-I, 1O, 2I-J, 2L, 5G, 5I, others).

Reviewer #2

(Remarks to the Author)
The authors have addressed all my comments fully.

Reviewer #3

(Remarks to the Author)
The authors have satisfactorily addressed most comments in the revision.

The regulation of IL33 locus by STAT-3 is not yet convincing. The authors acknowledge that YODA1 might not be the ideal system and have performed CUT&Tag-qPCR with 0h and 6h stretch. Why not replace the YODA1 data (Fig S7) with genome wide data using 0h and 6h stretch? In addition, a genome browser track of the location of the regions selected for CUT&Tag-qPCR would be very helpful. Finally, I am wondering how qPCR could show regulation if in the sequencing data there is no signal e.g. at the promoter?

Version 2:

Reviewer comments:

Reviewer #1

(Remarks to the Author)
The authors have made commendable efforts to address the issues raised in my prior comments and from the other reviewers. These changes have addressed my concerns satisfactorily.

Reviewer #3

(Remarks to the Author)
I appreciate the authors efforts to strengthen the data linked to direct regulation of IL33 by STAT-3.
I agree with the authors that CUT&RUN is better suited than CUT&Tag to profile transcription factor binding due to potential tagmentation of open chromatin by pA-Tn5.

Unfortunately, as also stated by the authors, the presented quality of CUT&RUN data in the revision is not high, e.g. the promoter mark H3K4me3 does not show the expected enrichment at promoter regions and distal peaks (e.g. peak 1) would be characterized by absence of H3K4me3 (Reviewer Figure 1A, B). The STAT3 signal does not appear different between peak and non-peak regions. Higher signal at peaks regions in 7S could also be explained by overall stronger signal across the whole locus as shown in Reviewer Figure 1B. Based on this it is very difficult to draw any robust conclusions of STAT3 binding from the analysis of the presented data.
Related to the CUT&Tag data: The explanation that the lack of signal at the IL33 promoter is due to a bias in library amplification is not convincing. For me it rather raises the question about what is amplified in qPCR? The signal in S7c overall is very sparse and comparing the peak calls with the signal tracks does not match well. I acknowledge that these experiments are difficult for TF and even more challenging for p-TFs.
Because of this, the presented data do not convincingly show direct regulation of IL33 by STAT. Thus, I think all what could be concluded is that STAT might directly control IL33.

RE: Point-by-point response (NCOMMS-24-47968A)

Contents

Reviewer #1 (Remarks to the Author):

This is an original manuscript from Zhang and colleagues exploring the role of PIEZO1 on endothelial cells in mouse models of pulmonary fibrosis. Reporting a small snRNA-seq dataset and analyzing other public resources, they suggest that there are increased endothelial cells in IPF lungs with evidence of mechanical stress, and in several preclinical fibrosis models, suggest that endothelial-cell Piezo1 is a potential driver of this. Several conditional deletion models and ex-vivo studies suggest that endothelial cell specific Piezo1 activation promotes fibrosis in an IL33 dependent manner. There has been limited study of the endothelium in pulmonary fibrosis pathogenesis and these studies offer potential new insights. There are a number of substantive analytical issues the authors need to address.

Major comments:

1) Figure 1: The assertion that there are increased endothelial cells in IPF lungs is at odds with considerable prior work and assessment of histopathology. These results are likely an artifact of small numbers, sampling methods, and statistical treatment.The resolution of annotation of this new snRNA-seq dataset is very low, and could be substantially improved using any of a number of public datasets as a reference.

A) The assertion that there are increased endothelial cells in IPF lungs is at odds with considerable prior work and assessment of histopathology.

Answer: We thank the reviewer for raising this important point. While traditional histopathological assessments may not always highlight endothelial cell proliferation, recent advances in single-cell RNA sequencing (scRNA-seq) have provided robust evidence for endothelial cell alterations in IPF. Below, we summarize key findings from three independent studies that support our assertion:

1. As showed in **(Figure 8J)**, Caporarello, Nunzia et al. identified a significant increase in pulmonary venous and systemic venous endothelial cells in IPF lungs through scRNA-seq analysis. The authors attributed this phenomenon to dysfunctional ERG signaling, which drives vascular aging and fibrosis.

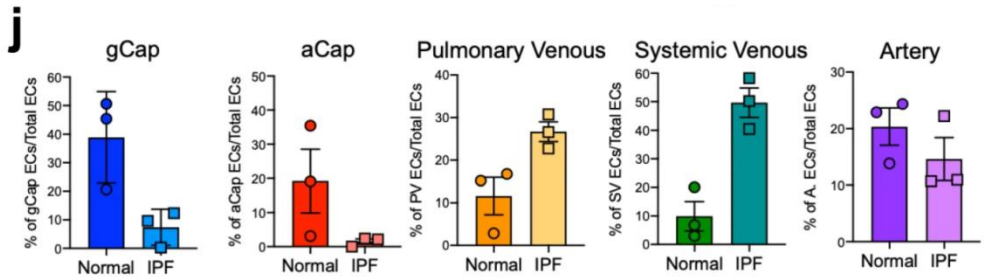

Relevant figure from this study:

Reference: Caporarello, Nunzia et al. Dysfunctional ERG signaling drives pulmonary vascular aging and persistent fibrosis. Nature communications vol. 13,1 4170. 25 Jul. 2022.

2. As showed in **(Figure 1C)**, Zhang et al. demonstrated a marked increase in the proportion of endothelial cells in IPF lungs compared to normal controls. Their scRNA-seq data further revealed distinct endothelial subpopulations contributing to fibrotic progression.

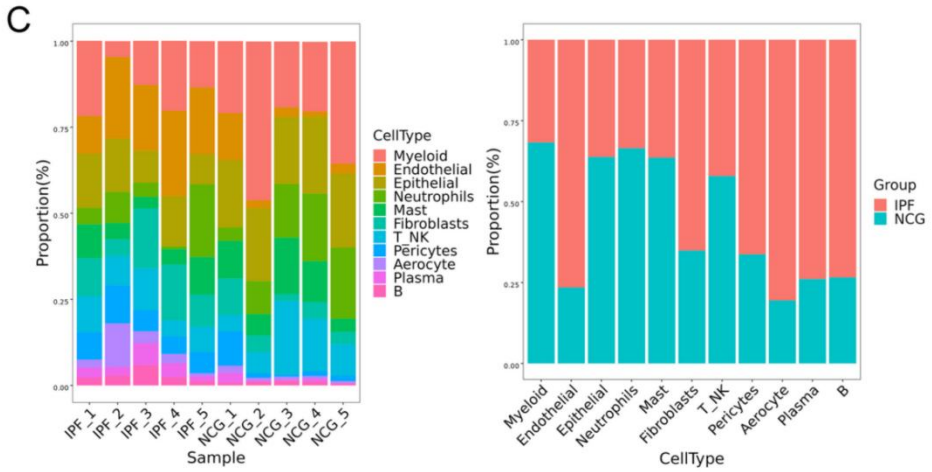

Relevant figure from the study:

Reference: Zhang T, et al. Single Cell RNA-Seq Identifies Cell Subpopulations Contributing to Idiopathic Pulmonary Fibrosis in Humans. J Cell Mol Med. 2025;29(3):e70402.

3. As showed in **(Fig. 1G)**, Jin et al. also reported elevated endothelial cell populations in IPF lungs via scRNA-seq. Their work emphasized the role of endothelial-fibroblast crosstalk in fibrosis.

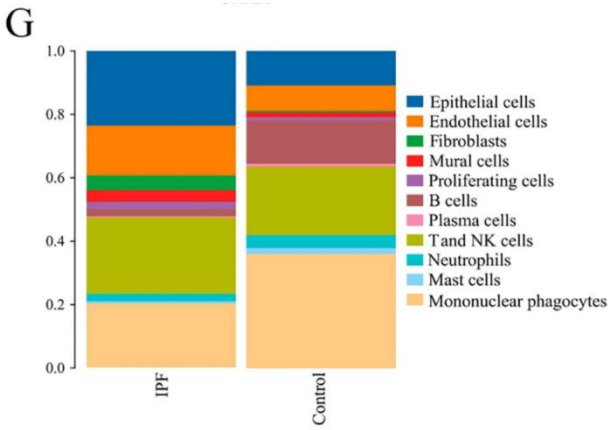

Relevant figure from the study:

Reference： Jin Chengji et al. Single-cell RNA sequencing reveals special basal cells and fibroblasts in idiopathic pulmonary fibrosis. Scientific reports vol. 14,1 15778. 9 Jul. 2024.

In conclusion: These studies underscore the dynamic changes in endothelial cells during IPF pathogenesis, as revealed by high-resolution scRNA-seq. While histopathology remains a cornerstone of IPF diagnosis, emerging technologies like scRNA-seq offer deeper insights into cellular heterogeneity and disease mechanisms.

B) The resolution of annotation of this new snRNA-seq dataset is very low, and could be substantially improved using any of a number of public datasets as a reference.

Answer: Thank you for your important comments. We have followed your very constructive advice to collect more patient samples for both control and IPF groups in all analyses, including single nucleus RNA-Seq (snRNA-Seq).We have referred a number of papers and re-annotated clusters using the published marker genes (Sikkema L et al., 2023 Nature medicine; Schupp JC, et al., 2021 Circulation). The revised results are shown below.

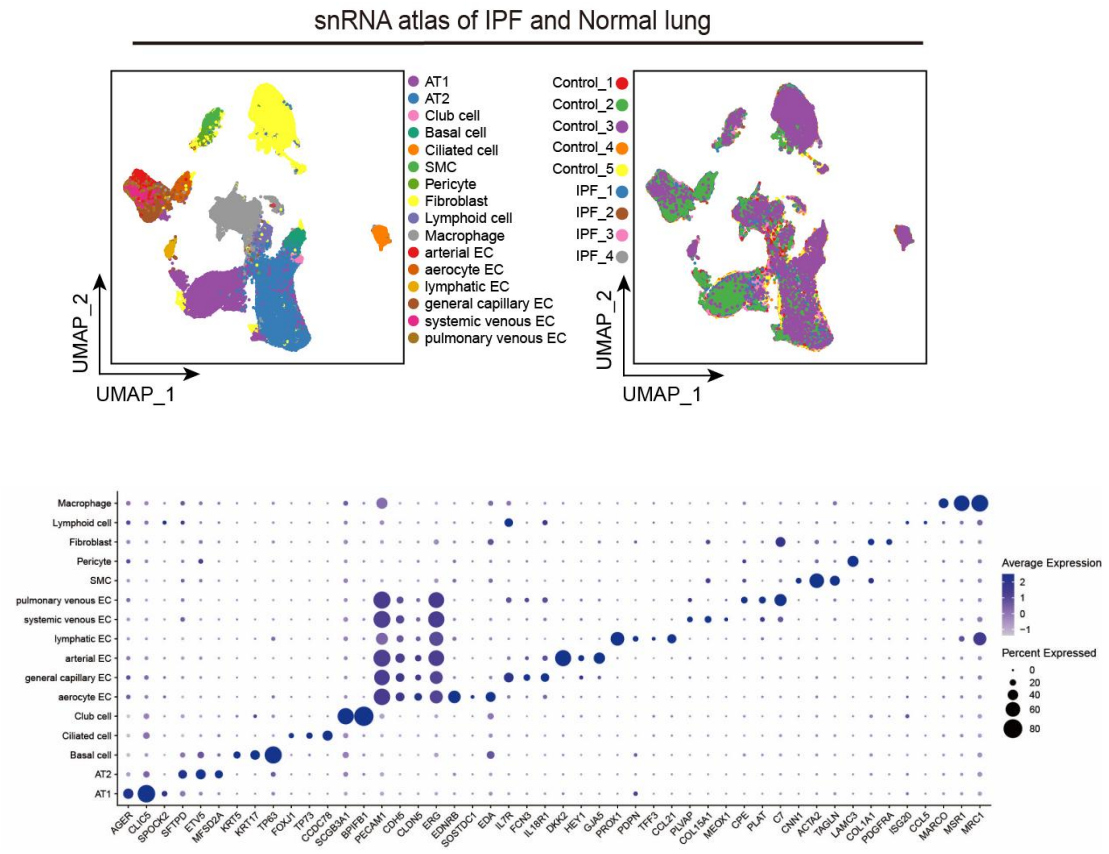

Figure to Reviewer 1: Subpopulation analysis was performed after single nucleus RNA sequencing (snRNA-Seq) of IPF patients and control subjects, **Data are shown in revised Fig.1B and Fig.S1C.**

References:

[1]. Schupp JC, et al. Integrated Single-Cell Atlas of Endothelial Cells of the Human Lung. Circulation. 2021 Jul 27;144(4):286-302.

[2]. Adams TS, et al. Single-cell RNA-seq reveals ectopic and aberrant lung-resident cell populations in idiopathic pulmonary fibrosis. Sci Adv. 2020 Jul 8;6(28):eaba1983.

C) This influences much of the downstream analysis. First, snRNA-seq of IPF and control lungs – lumping all endothelial cells for analysis of cell composition is not really meaningful (capillaries, venules, arterioles, etc are anatomically and functionally distinct).

Answer: Thanks so much for pointing out this very important point. We have reanalyzed the endothelial cells and devided into six subpopulations. The UMAP plot and dotplot of marker genes are shown.

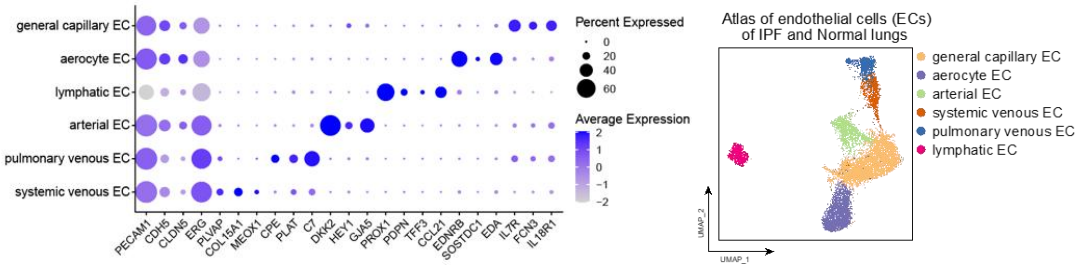

Figure to Reviewer 1: Endothelial cells (EC) were further subdivided into subpopulations including general capillary EC, aerocyte EC, arterial EC, systemic venous EC, pulmonary venous EC, and lymphatic EC, **Data are shown in revised Fig.S1B and Fig.1E.**

D) Second, assessment of cell composition from n of 3 samples is not robust (particularly as the authors could have assessed this from the meta-analyzed dataset presented later in the figure).

Answer: Thank you for this very important comment, and we have collected additional samples in response to your very constructive instructions. We have increased the number of normal samples to 5 and IPF samples to 4 (Fig.1B).

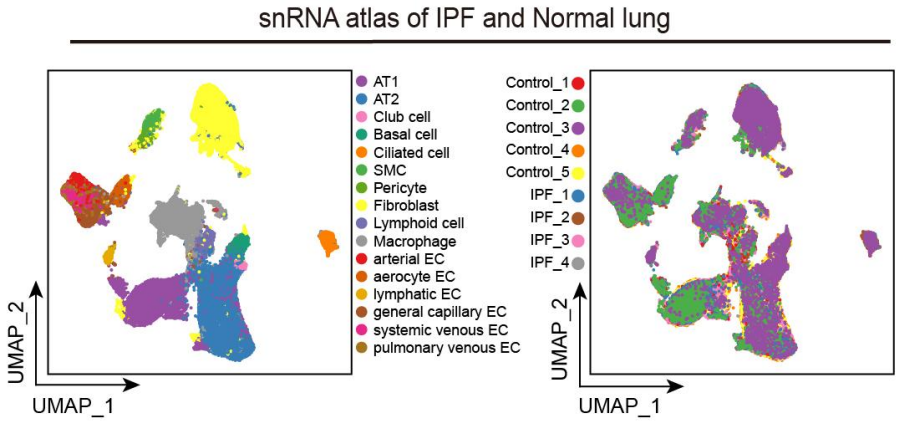

Figure to Reviewer 1: Subpopulation analysis was performed after single nucleus RNA sequencing (snRNA-Seq) of IPF patients (n=4) and control subjects (n=5), **Data are shown in revised Fig.1B.**

E) Third, since composition is a "zero-sum" scenario, Bayesian methods (i.e. propeller or others) are more appropriate.

Answer: Thank you for raising this important point. We have employed Propeller method to determine the proportions of cell subpopulations and validated the increase in endothelial cells.

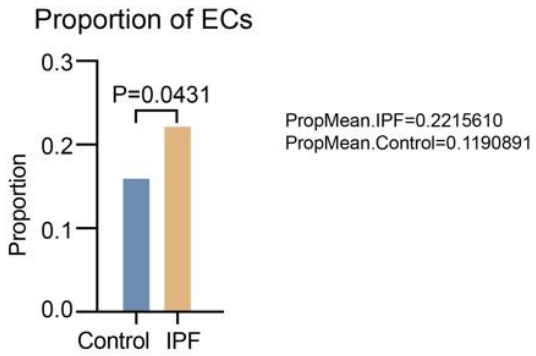

Figure to Reviewer 1: the increase of endothelial cells was verified by propeller method.

2) Figure 1: FVC-based classification as utilized by the authors reflects disease stage (not progression). The authors are not reporting an FVC rate of change (which would be an indicator of progression rate), but are reporting FVC which at one point in time is a measure of disease severity. Those with an FVC <50 do not necessarily have more rapidly progressive disease, they simply have had disease longer than those with and FVC >50%. This should be clarified in the text and figure legend.

Answer: Thank you for this insightful comment. Indeed, single time-point FVC measurements solely reflect disease severity rather than the annual rate of FVC decline — the gold-standard metric for evaluating disease progression. Our adoption of FVC $\leq$ 50% as the threshold is grounded in two key rationales:

Guideline Compliance: Primarily based on the 2022 clinical practice guidelines for adult IPF and progressive pulmonary fibrosis (PPF) jointly issued by ATS/ERS/JRS/ALAT, which classify FVC $\leq$ 50% as indicative of severe pulmonary dysfunction.

Program-Specific Criteria: Additionally guided by the diagnostic framework of the Inova Advanced Lung Disease Program, defining FVC $\leq$50% of predicted values as the threshold for severe physiological impairment.

These methodological justifications have been explicitly detailed in both the main text and figure legends(Raghu G et al., 2022 Am J Respir Crit Care Med; Pastre, J. et al., 2021 Respir Res).

References:

[1]. Raghu, G. et al. Idiopathic Pulmonary Fibrosis (an Update) and Progressive Pulmonary Fibrosis in Adults: An Official ATS/ERS/JRS/ALAT Clinical Practice Guideline. Am J Respir Crit Care Med. 2022 May 1;205(9):e18-e47.

[2]. Pastre, J. et al. Idiopathic pulmonary fibrosis patients with severe physiologic impairment: characteristics and outcomes. Respir Res. 2021 Jan 6;22(1):5.

3) Figure 1F: Numerous manuscripts have described COL15A1+/PLVAP+ "systemic-venous-like" endothelial cells as markedly more abundant in IPF lungs yet are not described in this figure – are these being misclassified as "capillary cells"?

Answer: We are sorry for the annotation in a low resolution. In our previously submitted manuscript, all the pulmonary and systemic venous ECs were annotated as venous ECs. We have re-annotated the endothelial cells using published marker genes including COL15A1 and PLVAP for systemic venous endothelial cells. The updated umap plot and dotplot of marker genes are shown below.

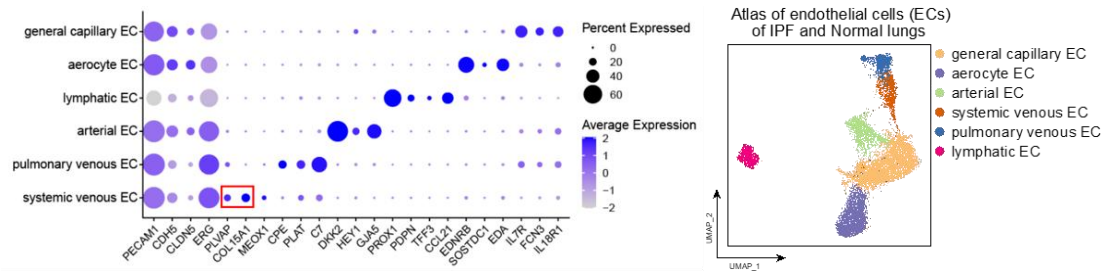

Figure to Reviewer 1: ECs were further subdivided into subpopulations including general capillary EC, aerocyte EC, arterial EC, systemic venous EC, pulmonary venous EC, and lymphatic EC, **Data are shown in revised Fig.S1B and Fig.1E.**

4) Lacking code availability or reporting of the genes which were used in the "mechanical stress" gene score, it is difficult to assess the robustness and reliability of this finding.

Answer: Thank you for this very important comment, and we have followed your highly constructive instruction and have uploaded relevant code which can be found at https://github.com/houruijiejerry/RuijieHou-Code. To obtain the mechanical gene sets for scoring, we performed enrichment analysis using the differential expressed genes between ECs of IPF samples and normal samples.

The mechanical gene set for human endothelial cell scoring: *EGFR, IL33, ITGA2, IGF1R, BMP6, IRF1, CASP8AP2, CD40, MAP2K4, MAPK8, BCL10, TMEM150C, TNFRSF1A, FAS, BAG3, CRADD, DAG1, PIEZO1, TNFRSF10A, CASP1, CASP8, F11R, TNFRSF8, SLC9A1, TLR3, CASP2, TLR4, GCLC, CHEK1, PTGER4, FADD, CASP5* GO:0071260, cellular response to mechanical stimulus.

The mechanical gene set for human endothelial cell scoring (public dataset): *PIEZO1, CCL2, HSP90B1, PIEZO2, SDC2, CTSL, GSTA1, MMP2, MMP9, CTNNB1, SDC1, MGST1, ITGAV, ACTG1, IL1R1, ASS1, NFKB1, CALM3, THBD, CALM2, GSTP1, RHOA, ACTB*

The mechanical gene set for endothelial cell of silica-induced mouse model scoring:

scRNA-seq data: *Cxcl12,Slc12a2,Gsn,Myc,Kit,Abl2,Htt,Itga2,Nfkbia,Cnn2,Thbs1,Slc9a1,Nfkb1,Ptn,Rest,Stra6,Pkd1,Tmem120a,Aqp1,Cav1,Atr,Tuba1a,Slc8a1,Nos3,Dag1,F11r,Atp8a2,Jup,Atp1a1,Got1,Rac1,Ptpn11,Mapk8,Pawr,Pkd2,Strbp,Shank3,Col6a1,Large1,Nrxn2,Tmem87a,Abhd12,Lck,Dmd,AU040320,Bace1,Piezo1,Piezo2,Fos,Ednra,Tlr4,Ripor2,Habp4,Smpd2,Mmp2,Raf1,Cxcr4,Serpine2,Cacnb3,Jun,Nrxn1,Ankrd2,Clcn6,* GO:0009612,response to mechanical stimulus.

scATAC-seq data: *Tmc1,Cradd,Kit,Slc12a2,Plec,Nfkbia,Got1,Gsn,Nos3,Nrxn2,P2rx3,F11r,Foxp2,Fos,Nfkb1,Pde2a,Pkd2l2,Gata4,Bag3,Raf1,Asic2,Htr2a,Shank3,Abhd12,Cd36,Slc9a1,Pawr, Strbp,Serpine2,Tlr4,Piezo2,Lck,Itga2,Fyn,Kcnq1,Cav1,Rac1,Cxcr4,Gsk3b,Ptprq,AU040320,Ryr2,Piezo1,Pkd1,Dag1,Etv1,Slc8a1,Abl2,Jun,* GO:0009612,response to mechanical stimulus.

The mechanical gene set for endothelial cell of bleomycin-induced mouse model scoring: *Piezo1, Piezo2,Atp1a1, Kit, F11r, Cxcl12, Cav1, Itga2, Pawr, Bag3, Hpn, Nos3, Pkd1, Jup, Shank3.*

5) Figures 2 and 3 – similar to the above comment, lumping all endothelial cells into a single population risks conflating changes in relative abundance of certain anatomically distinct populations with changes in chromatin accessibility and gene expression within a population. There are well-established marker genes that can discriminate endothelial cell subtypes into aCap, gCap, venule, arteriole and lymphatic populations at minimum to report these data.

Answer: Thank you for your suggestion. We have discriminated and annotated the endothelial cell subtypes with reported marker genes.

1) scRNA-seq data of silica mouse model:

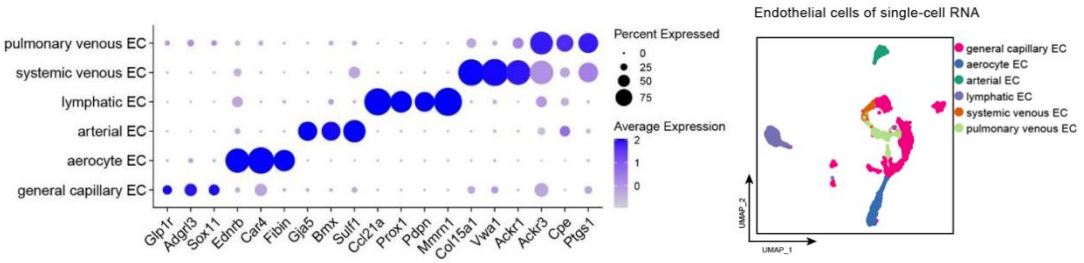

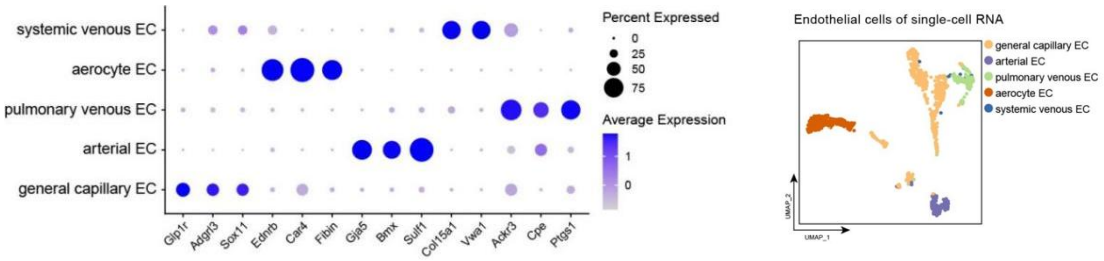

2) scRNA-seq data of bleomycin mouse model:

Figure to Reviewer 1: Endothelial cells (EC) were further subdivided into subpopulations including general capillary EC, aerocyte EC, arterial EC, systemic venous EC, pulmonary venous EC, and lymphatic EC in silica mouse model and bleomycin mouse model, Data are shown in revised **Fig.S3G, Fig.2G, Fig.S4J and Fig.S4I.**

6) Figure 3 – PIEZO2 is essentially not expressed in the vascular endothelium, so it is unclear what a ratio of Piezo1+/Piezo2+ cells would mean.

Answer: Thank you for highlighting this concern. We would like to clarify a terminological inaccuracy in our previous description. The intended meaning was to report the individual proportions of *PIEZO1*$^{+}$ and *PIEZO2*$^{+}$ cells within the endothelial cell population, rather than indicating a ratio between *PIEZO1* and *PIEZO2* expression levels.

7) Figure 4: Fibrosis assessments are reported as an "Inflammation Score" and "Relative Collagen Content" but no methods for these assessments are reported. Standard measures of fibrosis assessment (quantification of fibrotic area or Ashcroft score) in addition to hydroxyproline should be reported.

Answer: Thank you very much for your meticulous suggestions. We have followed your instruction to use new fibrosis assessment:

1) The severity of pulmonary inflammation was graded based on the following criteria:0, normal;1, inflammatory cells occupying 0%–10% of the entire tissue;2, inflammatory cells occupying 10%–40% of the entire tissue;3, inflammatory cells occupying 40%–70% of the entire tissue;4, inflammatory cells occupying 70%–100% of the entire tissue.

(2) For Sirius red staining or masson staining, Image J software was used to define the red areas (in Sirius red staining) or blue areas (in masson staining) in the tissue as positive areas. These areas were then outlined and their ratios to the entire field of view were calculated.

We also measured hydroxyproline levels, and assessed the protein levels of αSMA in lung tissue. The results are shown in the figure below.

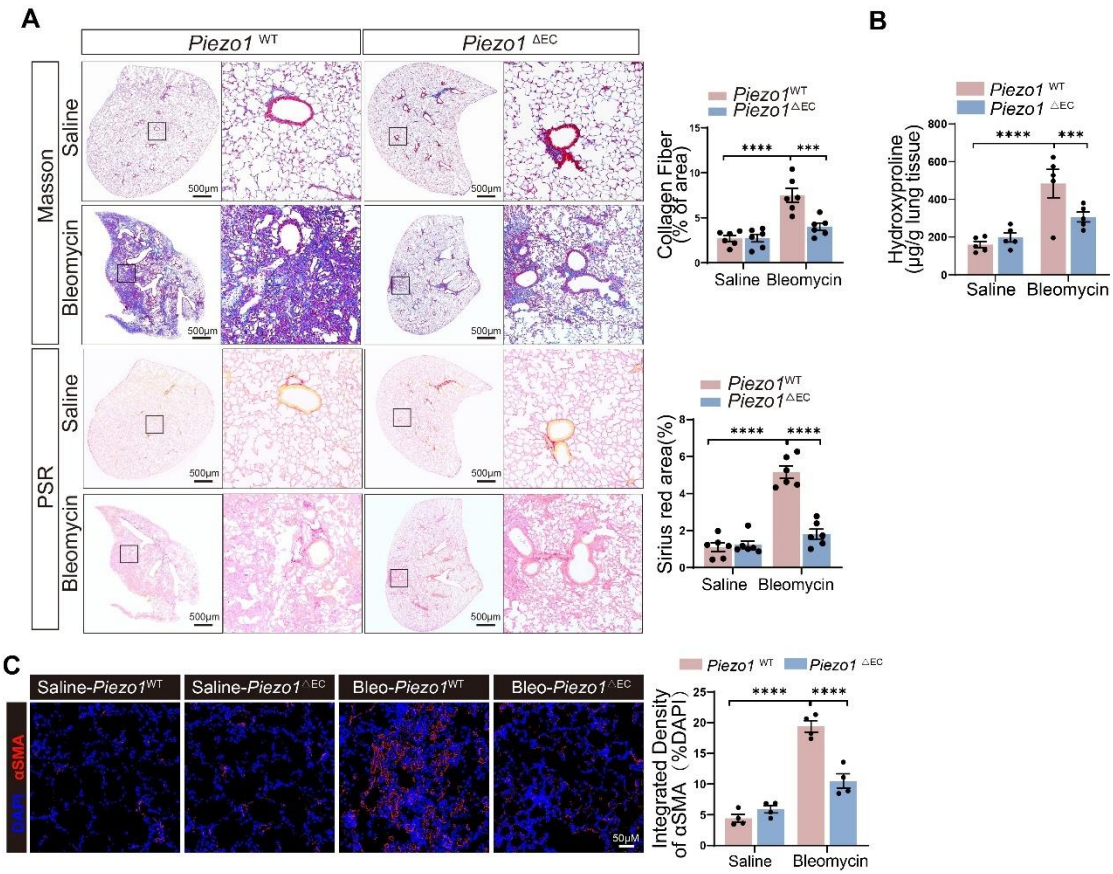

Figure to Reviewer 1: EC-specific deletion of Piezo1 in mice attenuated the fibrotic response in the BLM-induced mouse lung fibrosis model. **Data are shown in revised Fig.4C-F.**

(A)Representative images of Masson and Picro Sirius Red (PSR) staining in lungs of *Piezo1*^{WT} and *Piezo1*$^{\Delta EC}$ mice in BLM-induced fibrotic lungs. Quantification is shown on the right. N=6 mice per group. (B) The plot shows hydroxyproline amounts in lung tissues from *Piezo1*^{WT} and *Piezo1*$^{\Delta EC}$ mice in BLM-induced fibrotic lungs. N = 5 mice per group. (C) Immunofluorescent staining of αSMA(red) in lungs of *Piezo1*^{WT} and *Piezo1*$^{\Delta EC}$ mice in BLM-induced fibrotic lungs. Representative co-staining image of indicated mouse lungs is shown, and quantification (percentage of αSMA $^{+}$ integrated density relative to DAPI $^{+}$) is shown at the right (n=4). Error bars represent mean ± SEM. *P < 0.05, **P < 0.01, ***P < 0.001 and ****P < 0.0001.

8) No quantitative measurements of fibrosis are reported for the GsMTx4 or Yoda1 treatment studies in Figure 4I – any assertions of effects on fibrosis need to be supported by appropriate quantitative measures and statistical treatment.

Answer: We appreciate your advice and followed your constructive suggestion to analyze GsMTx4 or Yoda1 treatment studies, as shown in Fig.4H-4L to reviewer 1 below.

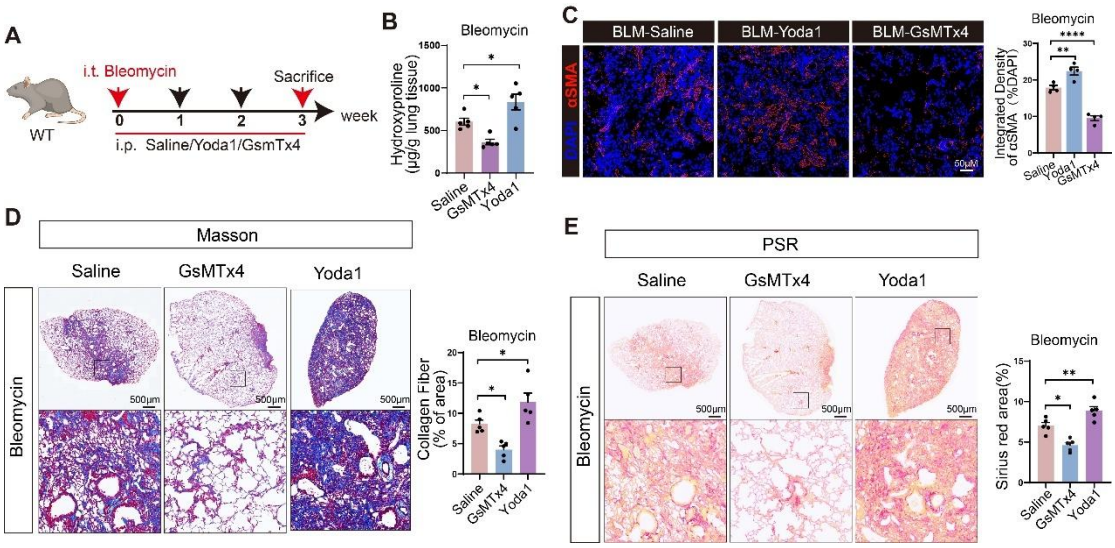

Figure to Reviewer 1: YODA1 and Gsmtx4 affect the fibrotic response in the bleomycin-induced mouse lung fibrosis model. **Data are shown in revised Fig.4G-4K.**

(A) The schematic illustrates the treatment of BLM-induced pulmonary fibrosis with the *PIEZO1* agonist Yoda1 and the antagonist GsMTx4. Mice were euthanized after 3 weeks. (B) The plot shows hydroxyproline amounts in lung tissues from mice in Yoda1 or GsMTx4-induced via intraperitoneal injection (n = 5). (C) Immunofluorescent staining of αSMA(red) in fibrotic lungs of mice in Yoda1 or GsMTx4-induced via intraperitoneal. Representative co-staining image of indicated

mouse lungs is shown, and quantification (percentage of αSMA $^{+}$ integrated density relative to DAPI $^{+}$) is shown at right (n = 4). (D-E) Representative images of Masson and PSR staining in fibrotic lungs of mice in Yoda1 or GsMTx4-induced via intraperitoneal. Quantification is shown at right (n = 5). Error bars represent mean ± SEM. *P < 0.05, **P < 0.01, ***P < 0.001 and ****P < 0.0001.

9) Figure 5 – cell communication analyses are really only informative at cell-type resolution – the finding that Piezo1 is correlated with Ackr1 (a specific marker of veins/venules) suggests that these findings overall reflect compositional differences within the endothelial cell population (rather than changes in cell-type specific expression related to Piezo1 expression).

Answer: Thank you for this insightful comment. We fully agree with the reviewer's perspective that cell communication analyses are most informative at the cell-type resolution. Regarding the observed correlation between *Piezo1* and *Ackr1* (a specific marker of veins/venules), we concur that this likely reflects compositional differences within the endothelial cell population rather than cell-type specific expression changes related to Piezo1 expression. We have revised it in the manuscript.

10) Figure 5J – the image quality is very low and not interpretable.

Answer: Thank you very much for your suggestions. We have re-stained the lung tissues from pulmonary fibrosis patients and fibrotic mice for IL-33.The results are shown in the figure below:

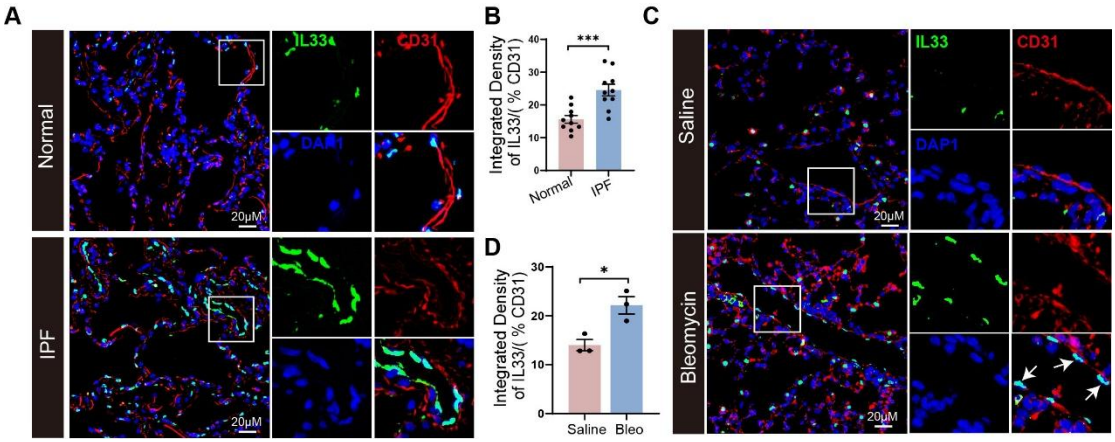

Figure to Reviewer 1: Expression of IL-33 in endothelial cells of fibrotic patient lungs and BLM-induced mouse fibrotic lungs. **A-B Data are shown in revised Fig.5H., while C-D are presented here exclusively.**

(A-B) Immunofluorescent staining showing the expression of IL-33 (green) in IPF

andnormal lungs. Co-staining of endothelial marker CD31 (red) was conducted. Quantification (percentage of IL-33+ integrated density relative to CD31+) is shown at the right (n=10). (C-D) Immunofluorescent staining of IL-33(green) in mouse fibrotic lungs. Co-staining of endothelial marker CD31(red) was conducted. Representative co-staining image of indicated mouse lungs is shown, and quantification (percentage of IL-33+ integrated density relative to CD31 +) is shown at the left (n=3). Error bars represent mean ± SEM. *P < 0.05 and ***P < 0.001.

11) Figure 6 – same comment as #7 – results regarding fibrosis need to be supported by standard, validated, methods for quantification of fibrosis.

Answer: We have followed your constructive comments to use new fibrosis assessment and revised it in the manuscript.The results are shown in the figure below:

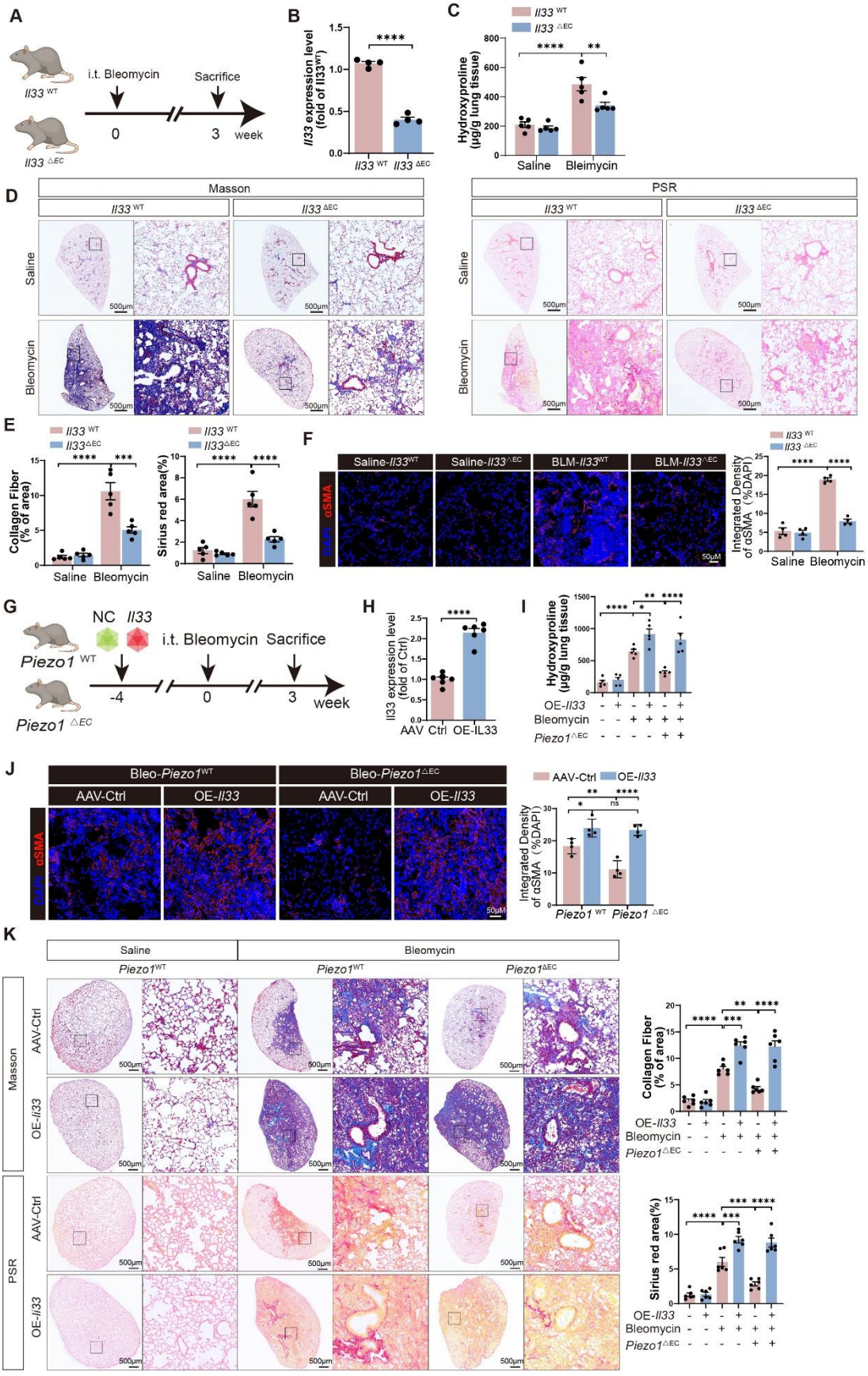

Figure to Reviewer 1: EC-specific deletion of Il-33 in mice attenuated the fibrotic response in the BLM-induced mouse lung fibrosis model. **Data are shown in revised Fig.6A-K**

(A) The schematic illustrates a BLM-induced lung fibrosis model established via tracheal administration in *Il-33*^{WT} and *Il-33*$^{\Delta EC}$ mice. (B) Quantification of *Il-33* mRNA in lung ECs of control *Il-33*^{WT} and *Il-33*$^{\Delta EC}$ mice (n = 4). (C) The plot shows hydroxyproline amounts in lung tissues from *Il-33*^{WT} and *Il-33*$^{\Delta EC}$ mice in BLM-induced fibrotic lungs(n = 5). (D-E) Representative images of Masson and PSR stainings in lungs of *Il-33*^{WT} and *Il-33*$^{\Delta EC}$ mice in BLM-induced fibrotic lungs(D). Quantification is shown on figure E (n = 5). (F) Immunofluorescent staining of αSMA(red) in lungs of *Il-33*^{wt} and *Il-33*$^{\Delta EC}$ mice in BLM-induced fibrotic lungs. Representative staining image of indicated mouse lungs is shown, and quantification (percentage of αSMA^{+} integrated density relative to DAPI^{+}) is shown at right (n = 4). (G) The schematic illustrates an EC-specific *Il-33* overexpression model was created using an adenoassociated virus (AAV) delivery system. The experimental protocol included: delivering AAV via trachea to *Piezo1*$^{\Delta EC}$ and *Piezo1*^{WT} mice for 4 weeks of pretreatment, followed by bleomycin administration in the 4th week, and euthanizing mice in the 7th week for lung tissue collection and further analysis. (H) The mRNA levels of *Il-33* in mouse ECs after injection of AAV-OE-*Il-33*. *Il-33* overexpression in lung ECs was achieved using Adeno-associated virus (AAV) system by EC-selective Tie1 promoter (n = 3). (I) The plot shows hydroxyproline amounts in lung tissues from *Piezo1*^{WT} and *Piezo1*$^{\Delta EC}$ injected with AAV-control(AAV-NC) and AAV-OE *Il-33* (n = 5). (J) Immunofluorescent staining of αSMA(red) in fibrotic lungs of *Piezo1*^{WT} and *Piezo1*$^{\Delta EC}$ injected with AAV-control(AAV-NC) and AAV-OE *Il-33*. Representative staining image of indicated mouse lungs is shown, and quantification (percentage of αSMA^{+} integrated density relative to DAPI^{+}) is shown at right (n = 4). (K) Representative images of Masson and PSR stainings in fibrotic lungs of *Piezo1*^{WT} and *Piezo1*$^{\Delta EC}$ injected with AAV-control(AAV-Ctrl) and AAV-OE-*Il-33*. Quantification is shown at right (n = 5). Error bars represent mean ± SEM. *P < 0.05, **P < 0.01, ***P < 0.001 and ****P < 0.0001

Minor comments:

1) Figure 2E: ILC's should not express Cd3e, the authors should check this annotation and/or evaluate ambient RNA contamination

Answer: We are sorry for the inaccurate annotation. We have re-annotated the data, and cells annotated as "ILC", are actually T cells.

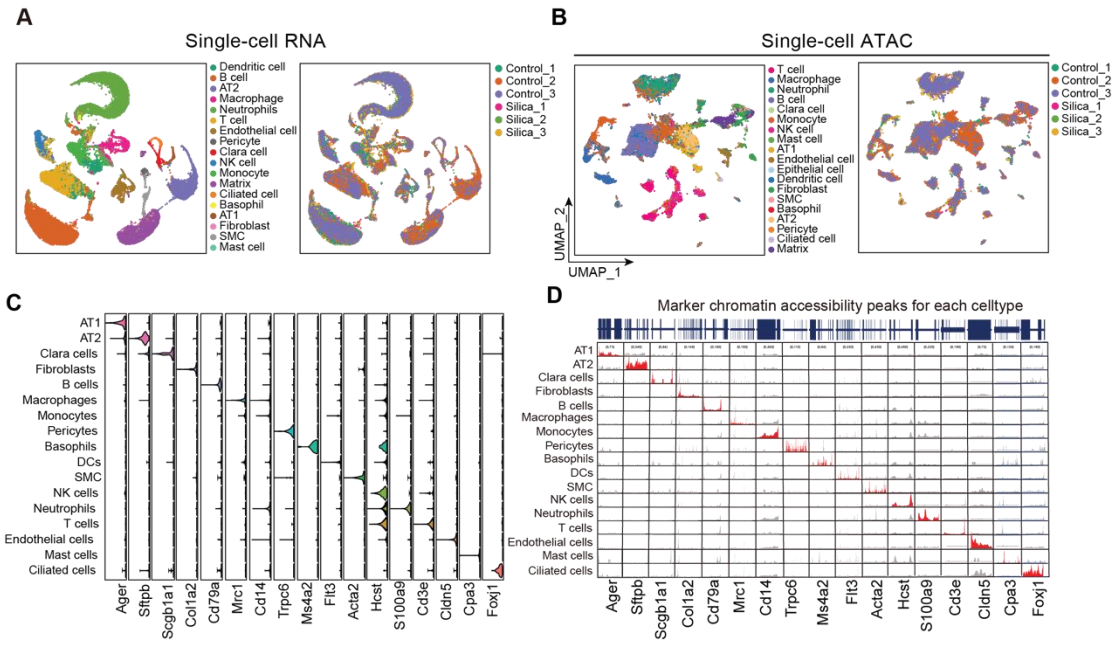

Figure to Reviewer 1: Single-Cell Holographic Analysis for SiO2 -Induced Mouse PF Model. **Data are shown in revised Fig.2C-F.**

(A) SiO2 UMAP plots of lung tissue scRNA-seq data from SiO2 model and control mice, colored by cell type. The UMAP plots depict various lung cell subpopulations, including Dendritic cells, B cells, AT2 cells, Macrophages, Neutrophils, T cells, Endothelial cells, Pericytes, Clara cells, NK cells, Monocytes, Fibroblasts, Ciliated cells, Basal cells, Mast cells, Matrix, and Smooth Muscle cells. (B) UMAP plot of scATAC-seq cell populations with with subpopulations annotated based on scRNA-seq analysis. (C) Violin plots showing lung cell type labeling of scRNA-seq data from SiO2 model and control mice. (D) In scATAC-seq data from SiO2 model and control mice, peaks for genes such as *Ager, Sftpb, Scgb1a1, Col1a2, Cd79a, Mrc1, Cd14, Trpc6, Ms4a2, Flt3, Acta2, Hcst, S100a9, Cd3e, Cldn5, Cpa3,* and *Foxj1* were identified in genomic regions typically for each subcelltype.

2) Results for Figure 3: "To investigate the subcellular distribution of PIEZOs in ECs, we analyzed human lung ECs using scRNA-seq bubble plots" – semanic point, but "bubble plots" are a visualization tool, not an analysis, and they report cellular (not "subcellular") expression.

Answer: Thank you for raising this important point. Bubble plots are indeed a visualization tool rather than a statistical analysis method. We have revised the wording and additionally performed t-tests for statistical analysis, illustrating the proportions of *PIEZO1* and *PIEZO2* separately through bar charts.

Reviewer #2 (Remarks to the Author):

This paper by Zhang, Zhang, Gui, Xia et al., looks at the role of endothelial PIEZO1 channels in the development of pulmonary fibrosis in two animal models. Using a Cre-lox strategy to specifically delete Piezo1 from endothelial cells they link PIEZO1 to the fibrotic cascade and attempt to link these effects to IL-33. Despite the raft of bioinformatics approaches the attempts to link this directly to mechanical stress are poorly fleshed out, for example a reader is still left with the question of exactly what cue is stimulating ECs in response to bleomycin or SiO2 to drive pulmonary fibrosis? This seems like a key question that the authors do a poor job of discussing. In addition, the use of PIEZO1 pharmacology is also rudimentary and there is no discussion of the off-target effects of GsMTx-4 or the fact that Yoda-1 drives cellular Ca2+ signalling that is spatio-temporally different from the mechanical activation of PIEZO1 (this is especially important for the in vitro experiments). Despite this, the data from KO mice and human datasets is compelling that PIEZO1 in ECs plays a role in the development of pulmonary fibrosis. The effects on IL-33 are strong and PIEZO1-dependent providing high level confidence that a PIEZO1-IL-33 pathway is at play in these disease models. I have a number of points below that require addressing prior to publication especially related to the in vitro experiments in HUVEC.
Just a general point the lack of line numbering makes reviewing arduous!

A) Despite the raft of bioinformatics approaches the attempts to link this directly to mechanical stress are poorly fleshed out, for example a reader is still left with the question of exactly what cue is stimulating ECs in response to bleomycin or SiO2 to drive pulmonary fibrosis? This seems like a key question that the authors do a poor job of discussing.

Answer： Thank you for your insightful comment. We appreciate the opportunity to clarify the mechanisms by which bleomycin and SiO2 induce fibrosis through mechanical disruption. Below, we provide a detailed explanation addressing the specific points raised:

Notably, in the acute phase, these stimuli firstly cause a direct damage on AT2 cells, which are pivotal for surfactant production and alveolar tension maintenance, leading to surfactant dysfunction and aberrant mechanical forces27. Concurrently, epithelial cell death and alveolar collapse further disrupt local mechanical equilibrium, exacerbating parenchymal stress(Snijder J et al., 2019 Expert Rev Respir Med). Moreover, these stimuli induce the acute inflammatory response and alveolar edema, which further cause the epithelial cell and endothelial cell injury and dysfunction and

amplifies mechanical dysregulation(Moeller A et al., 2008 Int J Biochem Cell Biol). Additionally, it have been reported pro-inflammatory cytokines such as IL-1β can directly induce expression of mechanosensitive genes (e.g., PIEZO1)(Chen W et al., 2024 Tissue Cell). Tang et al. reported that impaired AT2 cells produce mechanical tension that leads to spatially regulated fibrosis, initiating a new chapter in understanding PF)(Sainz de Aja J et al., 2020 Cell) . An interesting study showed that mechanical stretch activates PIEZO1 in caveolae of AT1 cell to trigger ATP release, and which in turn stimulate the surfactant paracrine secretion from AT2 cells(Diem K et al., 2020 FASEB J).

During the fibrotic phase, excessive ECM deposition increases tissue stiffness, initiating a self-amplifying cycle of mechanical stress, which resulting in the activation of mechanosensitive pathways in ECs, fibroblasts and other resident cells and thereby further accelerating ECM remodeling and fibrosis(Nho RS et al., 2022 Am J Pathol).The resulting pulmonary fibrosis, combined with chronic hypoxia, drives pathological vascular changes including pulmonary hypertension(Ruffenach G et al., 2020 Respir Res). This aligns with findings by Chen et al. showing Piezo1 upregulation mediates high shear stress-induced pulmonary hypertension(Chen J et al.,2022 Thromb Res). Ultimately, chronic fibrosis leads to lung function decline, causing respiratory rhythm disruption and perpetuating abnormal mechanical forces.

We have revised the “Manuscript Discussion” section to include further elaboration **(Lines 407-418)**. The flowchart is as follows:

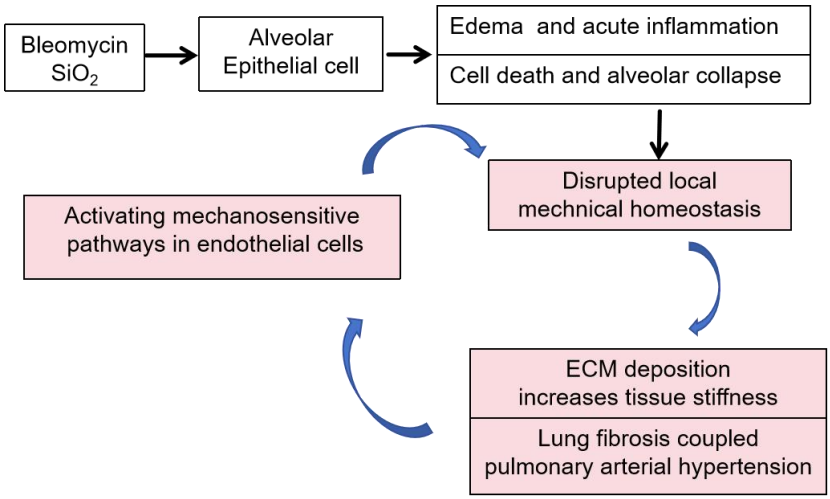

References:

[1]. Snijder J et al. Pulmonary fibrosis: a disease of alveolar collapse and collagen deposition. Expert Rev Respir Med. 2019 Jul;13(7):615-619.

[2]. Moeller A, et al. The bleomycin animal model: a useful tool to investigate treatment options for idiopathic pulmonary fibrosis? Int J Biochem Cell Biol. 2008;40(3):362-82.

[3]. Chen W, et al. Elucidating the mechanism of IL-1β-Mediated Piezo1 expression regulation of chondrocyte autophagy and apoptosis via the PI3K/AKT/mTOR signaling Pathway. Tissue Cell. 2024 Feb;86:102291.

[4]. Sainz de Aja J, et al. May the (Mechanical) Force Be with AT2. Cell. 2020 Jan 9;180(1):20-22.

[5]. Diem K,et al, Winokurow N, Schumacher S, Kranz C, Frick M. Mechanical stretch activates piezo1 in caveolae of alveolar type I cells to trigger ATP release and paracrine stimulation of surfactant secretion from alveolar type II cells. FASEB J. 2020 Sep;34(9):12785-12804.

[6]. Nho RS, et al. Biomechanical Force and Cellular Stiffness in Lung Fibrosis. Am J Pathol. 2022 May;192(5):750-761.

[7]. Ruffenach G, et al. Pulmonary hypertension secondary to pulmonary fibrosis: clinical data, histopathology and molecular insights. Respir Res. 2020 Nov 18;21(1):303.

[8]. Chen J, et al. Upregulation of mechanosensitive channel Piezo1 involved in high shear stress-induced pulmonary hypertension. Thromb Res. 2022 Oct;218:52-63.

B) In addition, the use of PIEZO1 pharmacology is also rudimentary and there is no discussion of the off-target effects of GsMTx-4 or the fact that Yoda-1 drives cellular Ca2+ signalling that is spatio-temporally different from the mechanical activation of PIEZO1 (this is especially important for the in vitro experiments).

Answer: Thank you for your valuable feedback on the pharmacological approaches targeting PIEZO1 in our study. We fully acknowledge the reviewer's concerns regarding the potential off-target effects of GsMTx-4 and the limitations of using Yoda-1, particularly its spatiotemporal specificity in mimicking mechanical activation of PIEZO1.

We agree that employing Yoda-1 to simulate mechanical activation of PIEZO1 represents a preliminary methodological approach. To address this limitation, we conducted additional experiments to directly evaluate the role of mechanical forces in

activating the PIEZO1 pathway. Specifically, the following experiments were added in Figure 7:

Stiffness modulation assays: By altering extracellular matrix stiffness, we modeled the mechanically rigid microenvironment observed during pulmonary fibrosis progression.

Endothelial cell stretch assays: Cyclic mechanical stretching devices were applied to simulate periodic stress generated by alveolar respiratory motion.

These experiments provide physiologically relevant models of mechanical forces and demonstrate that mechanically activated PIEZO1—independent of pharmacological agents—directly induces the expression of pro-fibrotic factors such as IL-33. These results complement the pharmacological data and offer robust evidence supporting the role of mechanical forces in pulmonary fibrosis.**We discussed it in manuscript from line 447-464.**

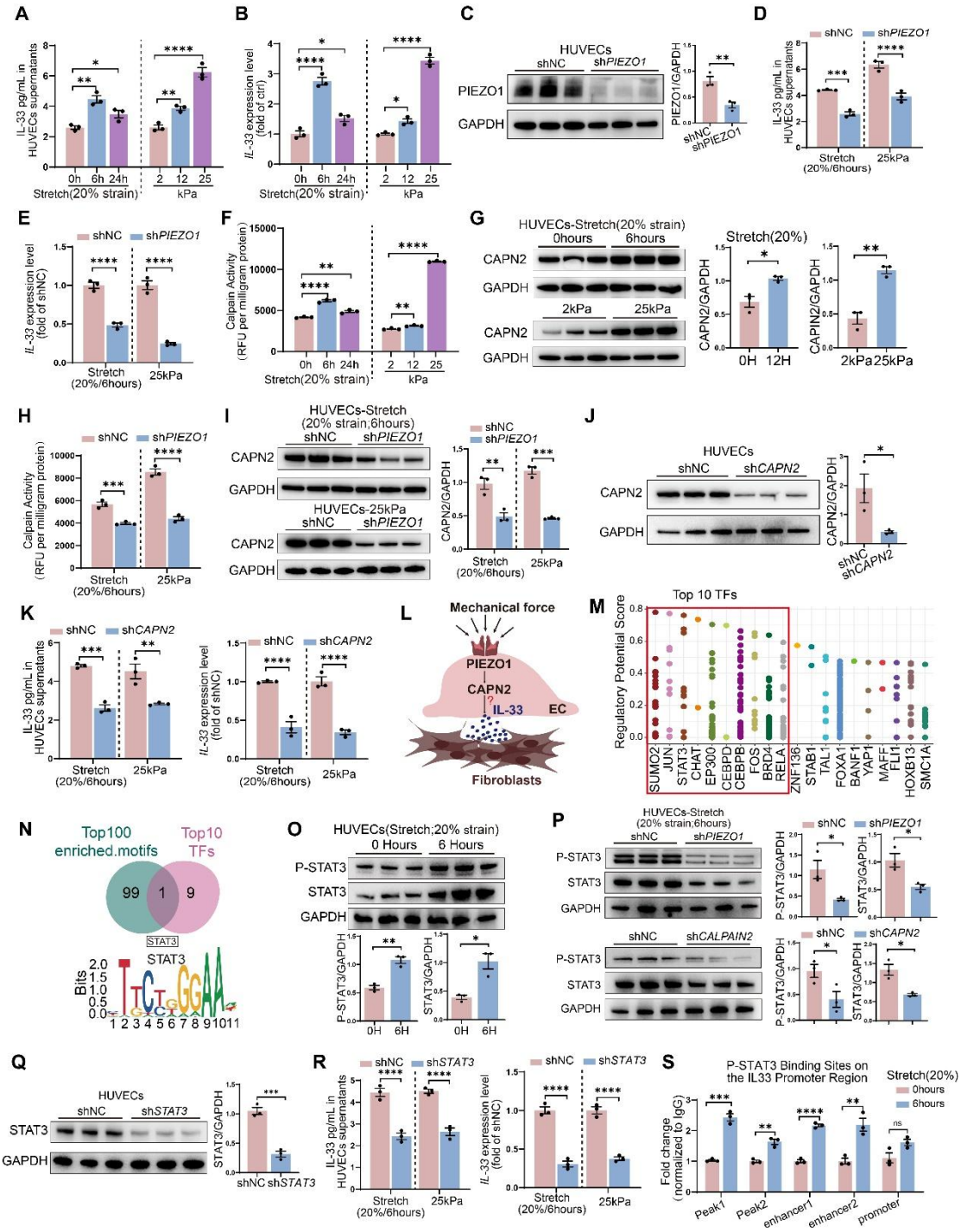

Figure to Reviewer 2: PIEZO1 upregulates IL-33 expression in HUVECs via the CAPN2-STAT3 axis. **Data are shown in revised Fig.7A-S.**

(A-B) The levels of IL-33 in HUVECs supernatants detected by ELISA(A), and the mRNA levels of IL-33 in HUVECs detected by qPCR(B). The HUVECs treated with stretch (20%) for 0, 6 and 24 hours and were cultured on substrates of 2 kPa ,12 kPa and 25 kPa for 24 hours (n = 3). (C) Protein levels of PIEZO1 in HUVECs treated

with shRNA targeting PIEZO1 (shPIEZO1) (n = 3). (D-E) The levels of IL-33 in HUVECs supernatants detected by ELISA(D), and the mRNA levels of IL-33 in HUVECs detected by qPCR(E). The HUVECs were treated with stretch (20%) for 6 hours and cultured on substrates of 2 kPa and 25 kPa for 24 hours after transduced with shPIEZO1 for 48 hours (n = 3). (F-G) The HUVECs treated with stretch (20%) for 0 ,6 and 24 hours and were cultured on substrates of 2 kPa ,12 kPa and 25 kPa for 24 hours. The calpain activity(F) and the protein levels of CAPN2(G) in HUVECs were detected (n = 3). (H-I) The HUVECs were treated with stretch (20%) for 6 hours and cultured on substrates of 2 kPa and 25 kPa for 24 hours after transduced with shPIEZO1 for 48 hours. The Calpain activity(H) and the protein levels of CAPN2(I) were detected (n = 3). (J) The protein levels of CAPN2 in HUVECs were treated with shRNA targeting CAPN2 (shCAPN2) (n = 3). (K) The levels of IL-33 in HUVECs supernatants detected by ELISA(left), and the mRNA levels of IL-33 in HUVECs detected by qPCR(right). The HUVECs were treated with stretch (20%) for 6 hours and cultured on substrates of 2 kPa and 25 kPa for 24 hours after transduced with shCAPN2 for 48 hours (n = 3). (L) Schematic showing the proposed mechanisms regulating paracrine expression of IL-33. (M) Cistrome database analysis predicts STAT3 as a key transcription factor in the regulation of IL-33 expression. (N) Venn diagrams indicating that the top 100 motifs in ECs of BLM-treated mice intersect with the top 10 transcription factors. (O) The HUVECs treated with stretch (20%) for 0 and 6 hours. The protein levels of P-STAT3 and STAT3 in HUVECs were detected (n = 3). (P) The protein levels of P-STAT3 and STAT3 in HUVECs were treated with stretch (20%) for 6 hours after transduced with shPIEZO1(up) and shCAPN2(down) for 48 hours (n = 3). (Q) The protein levels of STAT3 in HUVECs treated with shRNA targeting STAT3 (shSTAT3) (n = 3). (R) The levels of IL-33 in HUVECs supernatants detected by ELISA (left), and the mRNA levels of IL-33 in HUVECs detected by qPCR (right). The HUVECs were treated with stretch (20%) for 12 hours and cultured on substrates of 2 kPa and 25 kPa for 24 hours after transduced with shSTAT3 for 48 hours (n = 3). (S) Fold enrichment of P-STAT3 binding to the promoter region in HUVECs, as determined by Cut&Tag-qPCR. HUVECs were subjected to 20% stretch for 6 hours. Data are presented as fold enrichment relative to unstretched controls, normalized to IgG (n = 3). Error bars represent mean ± SEM. *P < 0.05, **P < 0.01, ***P < 0.001 and ****P < 0.0001.

1) Why is the control haplo-insufficient – what's its genotype? I assume this is a typo.

Answer: Thank you for your suggestion. This was a typographical error on our part. In the animal experiments, we used *Piezo1* $^{loxP/loxP}$ (*Piezo1*^{WT}) and *Il33* $^{loxP/loxP}$ (*Il33* ^{WT})

as the control groups, and CreERT2 *Piezo1*$^{loxP/loxP}$ (*Piezo1*$^{\Delta EC)}$ and CreERT2 *Il33* $^{loxP/loxP}$ (*Il33*$^{\Delta EC}$) as the experimental groups.

2) PIEZO1 vs Piezo1 needs uniformity.

Answer: Thank you for your suggestion. We have corrected all the Piezo1 formats.

3) Figure 4B comes from isolated ECs or whole tissue? If whole tissue how is the reduction so profound given all other cell types express PIEZO1. Figure 4I lacks quantification shown in Figure 4D.

Answer: Thank you for your suggestion, Figure 4B illustrates the use of magnetic beads to sort endothelial cells from mice. We have recalculated Figure 4I

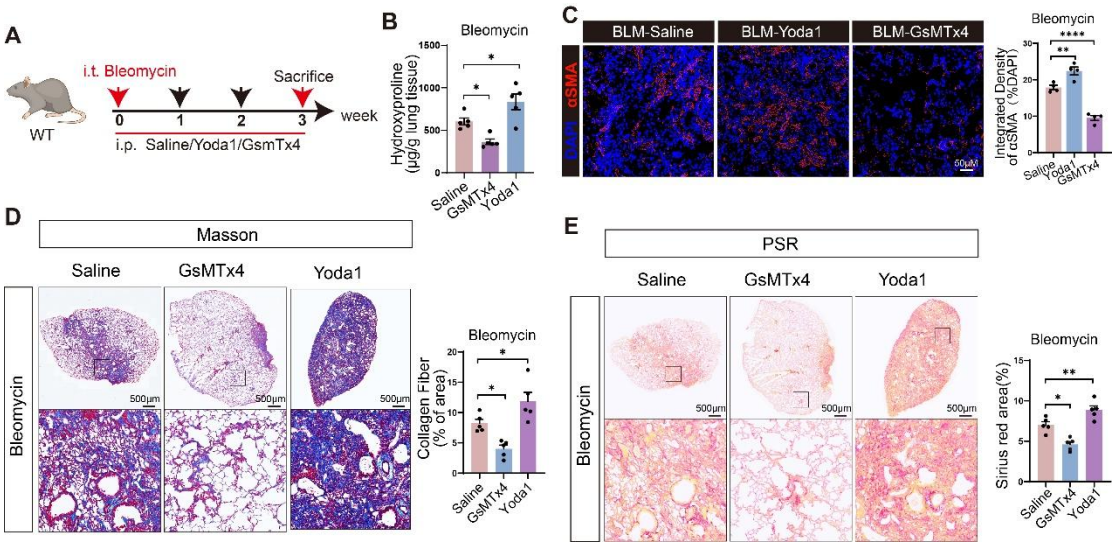

Figure to Reviewer 2: Yoda1 and Gsmtx4 affect the fibrotic response in the BLM-induced mouse lung fibrosis model. **Data are shown in revised Fig.4G-K.**

(A) The schematic illustrates the treatment of BLM-induced pulmonary fibrosis with the *PIEZO1* agonist Yoda1 and the antagonist GsMTx4. Mice were euthanized after 3 weeks. (B) The plot shows hydroxyproline amounts in lung tissues from mice in Yoda1 or GsMTx4-induced via intraperitoneal injection (n = 5). (C) Immunofluorescent staining of αSMA(red) in fibrotic lungs of mice in Yoda1 or GsMTx4-induced via intraperitoneal. Representative co-staining image of indicated mouse lungs is shown, and quantification (percentage of αSMA $^{+}$ integrated density relative to DAPI $^{+}$) is shown at right (n = 4).(D-E) Representative images of Masson and PSR staining in fibrotic lungs of mice in Yoda1 or GsMTx4-induced via intraperitoneal. Quantification is shown at right (n = 5). Error bars represent mean ± SEM. *P < 0.05, **P < 0.01, ***P < 0.001 and ****P < 0.0001.

4) For Figure 7 a calpain assay would be much better than mRNA levels. It's not clear why Yoda1 would increase the mRNA levels of calpain2(or STAT3 – STAT3 also doesn't come up earlier in the omics sections). The pathway should be dictated by Ca2+ induced activation of calpain – in this scenario as a homeostatic mechanism one might expect a reduction in calpain levels under a sustained mechanical cue not an increase. Using Yoda1 as a surrogate for mechanical stress is fraught with danger as it induces spatio-temporal Ca2+ signalling that is wholly different to mechanically induced PIEZO1 signalling. In a mechanical response PIEZO1 signalling is localized to certain regions like focal adhesions (Chen et al., 2018 Neuron; Yao et al., 2022 Science advances) and is transient. This is very different from when yoda1 is added – which causes a tonic sustained elevation in intracellular Ca2+. It is necessary to show the same pathway in response to a relevant mechanical cue. The reason for this is that if you use Yoda1 in an in vitro system you can end up suggesting a pathway like seen in cardiac PIEZOs (Zhang et al., 2021 Hypertension) that ends up being incorrect (Yu et al., 2022 Nature Cardiovascular Research). At least a mechanical cue should be used to validate these findings (stretch, stiffness, shear stress etc). This links back to the major question of what cue is driving this signalling in these disease models!!

A) It's not clear why Yoda1 would increase the mRNA levels of calpain2 (or STAT3 – STAT3 also doesn't come up earlier in the omics sections).

Answer: We thank the reviewer for their insightful comment. Notably, Calpain activity is known to be regulated by *Piezo1* in endothelial cells and macrophages (Li, J. et al., 2014 Nature; He Y et al., 2022 Hypertension; Luo S et al., 2025Theranostics). Our observation of upregulated CAPN2 and STAT3 aligns with prior reports; for example, Xiaodong Zhao et al. demonstrated that Yoda1 treatment enhances both enzymatic activity and protein abundance of Calpain2 in human kidney epithelial cells (Zhao X et al., 2022 JCI Insight). We hypothesize that sustained calcium signaling downstream of *PIEZO1* activation drives this transcriptional upregulation, creating a potential positive feedback loop within the mechanosensitive pathway. Specifically, *PIEZO1*-mediated calcium influx may directly activate CAPN2 while simultaneously inducing its mRNA expression—a mechanism consistent with broader calcium-dependent regulation. Given these implications, we think it deserve a further study.

References:

[1]. Li J, et al. Piezo1 integration of vascular architecture with physiological force. Nature. 2014 Nov 13;515(7526):279-282.

[2]. He Y, et al. Myeloid Piezo1 Deletion Protects Renal Fibrosis by Restraining Macrophage Infiltration and Activation. Hypertension. 2022 May;79(5):918-931.

[3]. Luo S, et al. Piezo1 specific deletion in macrophage protects the progression of liver fibrosis in mice. Theranostics. 2023 Oct 2;13(15):5418-5434.

[4]. Zhao X, et al. Mechanosensitive Piezo1 channels mediate renal fibrosis. JCI Insight , (2022).

B) At least a mechanical cue should be used to validate these findings (stretch, stiffness, shear stress etc).

Answer: Thank you for your valuable suggestions. We apologize for not including data induced by tension, stiffness, and shear stress. We have analyzed the Calpain activity and the protein levels of CAPN2, STAT3, and P-STAT3 in cells subjected to tension and cultured on substrates of varying stiffness. The results show that tension and culture on substrates of different stiffness stimulate the expression of CAPN2 and P-STAT3. The results are shown in the figure below.

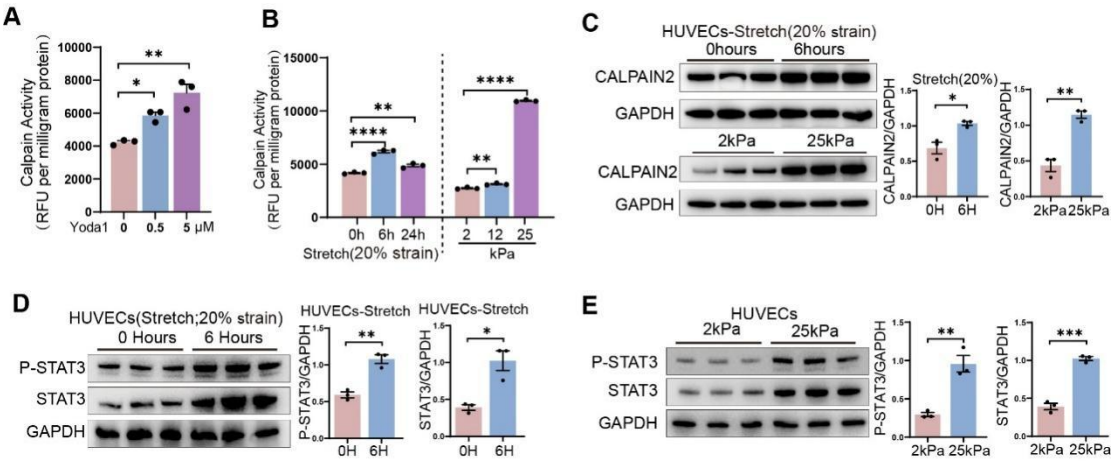

Figure to Reviewer 2: The effects of different mechanical stimuli on the expression of CAPN2 in HUVECs. **Data are shown in revised Fig.7F-G,7O and Fig.S7D.**

(A) HUVECs were treated with 0 μM, 0.5 μM and 5 μM PIEOZ1 agonist Yoda1 for 24 hours, and Calpain activity were detected. N=3 per group. (B-C) The HUVECs treated with stretch (20%) for 0,6 and 24 hours and were cultured on substrates of 2 kPa and 25 kPa for 24 hours. The calpain activity(A) and the protein levels of CAPN2(B) in HUVECs were detected. N=3 per group. (D-E) The HUVECs treated

with stretch (20%) for 0 and 6 hours and were cultured on substrates of 2 kPa and 25 kPa for 24 hours. The protein levels of P-STAT3 and STAT3 in HUVECs were detected. N=3 per group. Error bars represent mean ± SEM. *P < 0.05, **P < 0.01, ***P < 0.001 and ****P < 0.0001.

5) There's also no data that IL-33 is actually released. An ELISA showing PIEZO1-mediated release of IL-33 is really essential as generally speaking the paper is too reliant on mRNA levels to suggest mechanism.

Answer: Thank you for your valuable suggestions. We apologize for not including data from IL-33 release ELISA kits. We have re-analyzed the secretion and transcription of IL-33 in cells subjected to tension and cultured on substrates of different stiffness. The results are shown in the figure below.

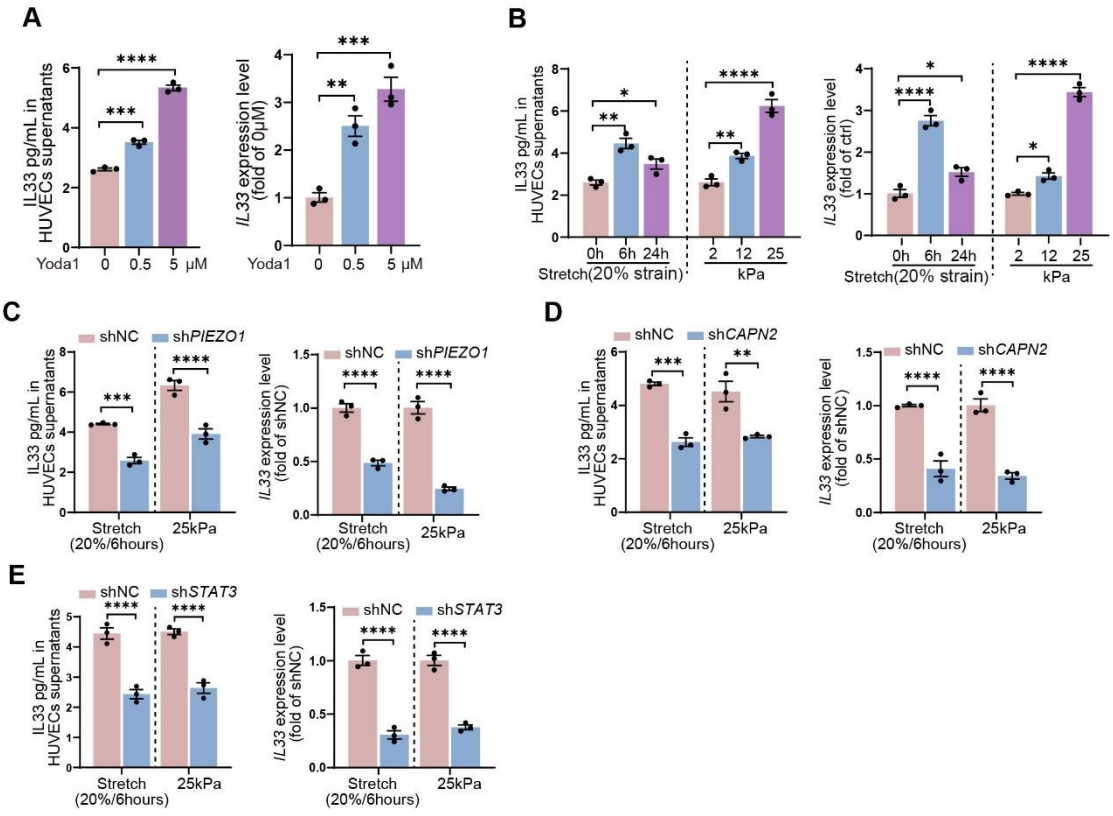

Figure to Reviewer 2: Different mechanical stimuli influence the expression of *CAPN2* in HUVECs via the *PIEZO1-CAPN2-STAT3* axis. **A are presented here exclusively; B-E are shown in revised Fig.7A-B,7D-E,7K,7R.**

(A) The levels of IL-33 in HUVECs supernatants detected by ELISA and the mRNA levels of *IL-33* in HUVECs detected by qPCR (right). The HUVECs treated with 0 μM, 0.5 μM and 5 μM *PIEOZ1* agonist Yoda1 for 24 hours. N = 3 per group. (B) The

levels of IL-33 in HUVECs supernatants detected by ELISA (left), and the mRNA levels of *IL-33* in HUVECs detected by qPCR (right). The HUVECs treated with stretch (20%) for 0, 6 and 24 hours and were cultured on substrates of 2 kPa ,12 kPa and 25 kPa for 24 hours. N = 3 per group. (C-E) The levels of IL-33 in HUVECs supernatants detected by ELISA (left), and the mRNA levels of *IL-33* in HUVECs detected by qPCR(right). The HUVECs were treated with stretch (20%) for 6 hours and cultured on substrates of 2 kPa and 25 kPa for 24 hours after transduced with sh*PIEZO1,* sh*CAPN2* and sh*STAT3* for 48 hours. N=3 per group. Error bars represent mean ± SEM. *P < 0.05, **P < 0.01, ***P < 0.001 and ****P < 0.0001.

Reviewer #3 (Remarks to the Author):

Zhang et al. present a study "Single-cell multiomics reveals endothelial mechanosensitive PIEZO1 coupling IL33 regulates the development of pulmonary fibrosis" that uncovers a molecular mechanism of pulmonary fibrosis (PF). PF is a lethal disease with limited treatment options. By analyzing sc/nRNA-seq and scATAC-seq data from human specimens and two mouse models (silica and Bleomycin induced) the study authors identify upregulation of genes linked to mechanosensation in endothelial cells. They identify PIEZO1 as top candidate and validate its role using genetic deletion in a mouse model and small molecule inhibition or activation. They could show that blocking or deleting PIEZO1 decreases fibrosis and activation resulted in increased fibrosis. Finally, they show that PIEZO1 couples to IL33 and activates a CAPN2-STAT3 signalling cascade.
This is an exciting, comprehensive and well executed study covering hypothesis generating single cell data and follow-up analysis using genetic mouse models and small molecules to validate predictions for the role of PIEZO1 and related signaling in PF.

I have a few comments that would need to be addressed:

1) According to Table S1 and S2 only 5 donors were profiled? Where does the sixth data point in the figures come from? Please clarify.

Answer: We are sorry for the missing information of the sixth donor. We have included all the information, including the missing part and the new information. **Data are shown in revised Table S1.**

2) What genes are in the MS Score? How was the statistic calculated in 1N, 2H, 2J. Per individual or per cell?

Answer: To obtain the mechanical gene sets for scoring of per cell, we performed enrichment analysis using the differential expressed genes between endothelial cells of IPF samples and normal samples.

The mechanical gene set for human endothelial cell scoring: *EGFR, IL33, ITGA2, IGF1R, BMP6, IRF1, CASP8AP2, CD40, MAP2K4, MAPK8, BCL10, TMEM150C, TNFRSF1A, FAS, BAG3, CRADD, DAG1, PIEZO1, TNFRSF10A, CASP1, CASP8, F11R, TNFRSF8, SLC9A1, TLR3, CASP2, TLR4, GCLC, CHEK1, PTGER4, FADD, CASP5* GO:0071260, cellular response to mechanical stimulus.

The mechanical gene set for human endothelial cell scoring (public dataset): *PIEZO1, CCL2, HSP90B1, PIEZO2, SDC2, CTSL, GSTA1, MMP2, MMP9, CTNNB1, SDC1, MGST1, ITGAV, ACTG1, IL1R1, ASS1, NFKB1, CALM3, THBD, CALM2, GSTP1, RHOA, ACTB*

The mechanical gene set for endothelial cell of silica-induced mouse model scoring:

scRNA-seq data: *Cxcl12,Slc12a2,Gsn,Myc,Kit,Abl2,Htt,Itga2,Nfkbia,Cnn2,Thbs1,Slc9a1,Nfkb1,Ptn,Rest,Stra6,Pkd1,Tmem120a,Aqp1,Cav1,Atr,Tuba1a,Slc8a1,Nos3,Dag1,F11r,Atp8a2,Jup,Atp1a1,Got1,Rac1,Ptpn11,Mapk8,Pawr,Pkd2,Strbp,Shank3,Col6a1,Large1,Nrxn2,Tmem87a,Abhd12,Lck,Dmd,AU040320,Bace1,Piezo1,Piezo2,Fos,Ednra,Tlr4,Ripor2,Habp4,Smpd2,Mmp2,Raf1,Cxcr4,Serpine2,Cacnb3,Jun,Nrxn1,Ankrd2,Clcn6,* GO:0009612,response to mechanical stimulus.

scATAC-seq data: *Tmc1,Cradd,Kit,Slc12a2,Plec,Nfkbia,Got1,Gsn,Nos3,Nrxn2,P2rx3,F11r,Foxp2,Fos,Nfkb1,Pde2a,Pkd2l2,Gata4,Bag3,Raf1,Asic2,Htr2a,Shank3,Abhd12,Cd36,Slc9a1,Pawr, Strbp,Serpine2,Tlr4,Piezo2,Lck,Itga2,Fyn,Kcnq1,Cav1,Rac1,Cxcr4,Gsk3b,Ptprq,AU040320,Ryr2,Piezo1,Pkd1,Dag1,Etv1,Slc8a1,Abl2,Jun,* GO:0009612,response to mechanical stimulus.

The mechanical gene set for endothelial cell of bleomycin-induced mouse model scoring: *Piezo1, Piezo2,Atp1a1, Kit, F11r, Cxcl12, Cav1, Itga2, Pawr, Bag3, Hpn, Nos3, Pkd1, Jup, Shank3.*

3) MS Score analysis shows an increase in PF in the silica model (2H, 2J), but in the Bleomycin model mostly Piezo1/2 are robustly regulated (3K). How can this be explained?

Answer: We sincerely apologize for the oversight in not listing the mechanosensitive differentially expressed genes (DEGs) in endothelial cells (ECs) between the silica- and bleomycin-induced fibrosis models, which may have caused confusion. To clarify, based on snATAC-seq analysis, the mechanosensitive gene set significantly enriched in the silica model includes: *Tmc1*, *Cradd*, *Kit*, *Slc12a2*, *Plec*, *Nfkbia*, *Got1*, *Gsn*, *Nos3*, *Nrxn2*, *P2rx3*, *F11r*, *Foxp2*, *Fos*, *Nfkb1*, *Pde2a*, *Pkd2l2*, *Gata4*, *Bag3*, *Raf1*, *Asic2*, *Htr2a*, *Shank3*, *Abhd12*, *Cd36*, *Slc9a1*, *Pawr*, *Strbp*, *Serpine2*, *Tlr4*, *Piezo2*, *Lck*, *Itga2*, *Fyn*, *Kcnq1*, *Cav1*, *Rac1*, *Cxcr4*, *Gsk3b*, *Ptprq*, *AU040320*, *Ryr2*, *Piezo1*, *Pkd1*, *Dag1*, *Etv1*, *Slc8a1*, *Abl2*, and *Jun*.

In the bleomycin model, mechanosensitive genes enriched include *Piezo1*, *Piezo2*, *Atp1a1*, *Kit*, *F11r*, *Cxcl12*, *Cav1*, *Itga2*, *Pawr*, *Bag3*, *Hon*, *Nos3*, *Pkd1*, *Jup*, and *Shank3*. Importantly, the BLM-associated mechanosensitive gene profile is not limited to *Piezo1* and *Piezo2*. The *Piezo1* and *Piezo2* highlighted **in Figure 3K** of the original manuscript represent the core consensus genes identified across multiple independent datasets (including the bleomycin mechanosensitive gene set), rather than being exclusive to a single model. We then used Venn diagram analysis to integrate bulk RNA-seq with a single multi-omics dataset, confirming the involvement of Piezo1 and Piezo2 in the pathogenesis of PF **(Figure 3J).**

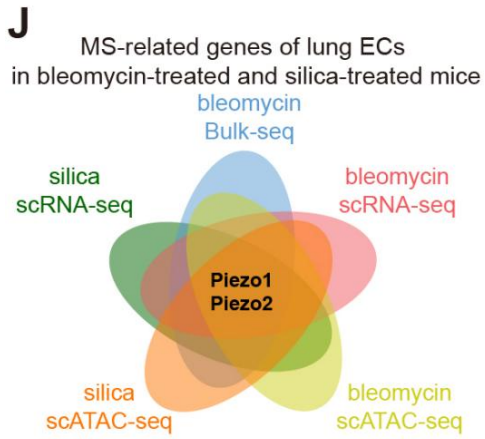

Figure to Reviewer 3: Venn diagram showing that *Piezo1* and *Piezo2* are co-regulated genes across bulk sequencing, scRNA-seq, and scATAC-seq data from the Silica-induced and BLM-induced mouse model. **Data are shown in revised Fig.3J.**

4) The scATAC-seq data lacks analytical details, e.g. how were cells filtered? How was peak calling performed? How was transcription factor motif enrichment performed? How was batch correction performed and doublets removed (also for scRNA data)?

Answer： We appreciate the reviewer's comment. We have provided a more detailed method to explain the analytical details.

For scATAC-seq data, cells were filtered using the following criteria: 1)3000<nCount_peaks< 50000; 2) pct_reads_in_peaks>15; 3) blacklist_ratio<0.05; 4)Nucleosome signal<4; 5) transcription start site (TSS) enrichment score>1. Batch effects were corrected using the Harmony. Peaks calling was performed using MACS2. Motif analysis was performed using Signac package mainly. Transcription factor (TF) binding motifs were downloaded from JASPAR database. Then TF

binding motifs were mapped to scATAC-seq peaks using AddMotifs function. RunChromVAR function was used for calculating motif deviation score. We performed GO enrichment analysis after differential accessibility analysis with FindMarkers function and obtained corresponding motifs using FindMotifs function. MotifPlot function was used to visualize motifs of peaks with different accessibility between groups.

For scRNA/snRNA-seq data, any single cell with less than 200 genes or more than 5000 genes, and cells with more than 25% mitochondrial genes were regarded as low quality cells and excluded. Possible doublets were detected using DoubletFinder and removed. Each dataset was log-normalized using the NormalizeData function. Genes with large differences in expression between cells were identified using the FindVariableFeatures function, and the data was scaled using ScaleData. Integrate each sample and correct batch effects using the Harmony.

5) Fig 2L "different thematic patterns of ECs" -> TF motif enrichment analysis? How was this analysis performed, which tool was used? Is this analysis performed on all ECs or differential accessible sites (same for Bleomyin analysis)? What about all the other motifs except STAT motif that were identified from the scATAC analysis?

Answer: We appreciate the reviewer's comment. We will address each of your questions point-by-point below.

1.The incorrect description "different thematic patterns of ECs" has been replaced by "TF motif enrichment analysis".

2.To perform motif analysis, transcription factor (TF) binding motifs were downloaded from JASPAR database. Then TF binding motifs were mapped to scATAC-seq peaks. Motif analysis was performed using Signac package.

3.Only the differential accessible sites between IPF and control samples were analyzed.

4 .We also identified other motifs from the scATAC analysis, but only the motifs of mechanical stress-related genes are shown.

6) 3G what exactly is displayed: Figure panel states motif and legend states an AUC score of mechanical stress genes.

Answer: We are sorry for the mismatch between legend and Figure panel, which has been corrected in the revised version. Figure 3G in the previous version was the result of AUCell scoring, which has been deleted in the latest version.

7) 7J there is no binding of STAT3 at the promoter region of IL33 on the tracks visible. The signal of STAT3 at most sites is lower after YODA1 treatment despite the model would suggest otherwise. Do all peaks have a STAT3 binding site?

Answer: We appreciate the reviewer's thoughtful comment and are grateful for the observations regarding the CUT&Tag seqencing data. Specifically, the result does not show STAT3 binding at the IL33 promoter region, and it is hard to distinguish the difference of binding signaling intensity between YODA1-treated and control groups. The challenge arises because these signals identified by CUT&Tag sequencing analysis were relatively weak, making it difficult to conclusively determine their validity.

To address this limitation, we conducted further validation using CUT&Tag-qPCR. We selected the promoter region and two additional enhancer sites annotated in the UCSC database, along with two putative STAT3 binding peaks identified from our CUT&Tag sequencing data. By performing CUT&Tag-qPCR on these sites, we aimed to provide more robust evidence for STAT3 binding..

Region	Genomic Coordinates (chr9)	Source	Validation Result
Peak1	6,149,365–6,149,765	Novel	Positive
Peak2	6,184,615–6,185,015	Novel	Positive
Enhancer1	6,185,024–6,185,424	UCSC	Positive
Enhancer2	6,195,974–6,196,374	UCSC	Positive
Promoter	6,215,585–6,215,985	UCSC	Positive

Additionally,we acknowledge the reviewer's valid concern regarding YODA1 as an imperfect mimic of pathological PIEZO1 activation. To address this limitation, we implemented complementary in vitro systems incorporating substrate stiffness modulation and mechanical stretch. These parallel approaches allow for more rigorous examination of STAT3's capacity to directly bind IL-33 regulatory regions under diverse mechanosensitive conditions.

As demonstrated in Fig. 7Q, STAT3 binding showed significant enrichment at Peak1, Peak2, Enhancer1, and Enhancer2, with a similar increasing trend observed in the promoter region following activation of mechanosensitive pathways by stiffness and stretch stimuli. These findings collectively suggest that mechanical stimuli promote STAT3 binding across multiple regulatory elements of the *IL-33* gene.

We appreciate the reviewer's insightful comment and will incorporate this clarification in the revised manuscript.

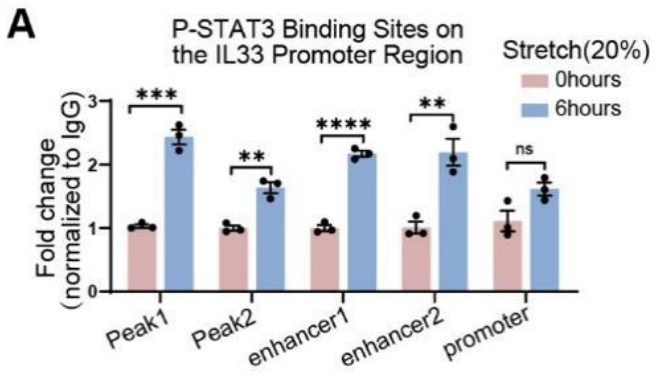

Figure to Reviewer 3: Cut&Tag-qPCR shows that mechanical stretch promotes the binding of P-STAT3 to the IL-33 promoter region in HUVECs. **Data are shown in revised Fig.7S.**

A) Fold enrichment of P-STAT3 binding to the IL-33 promoter region in HUVECs, as determined by Cut&Tag-qPCR. HUVECs were subjected to 20% stretch for 6 hours. Data are presented as fold enrichment relative to unstretched controls, normalized to IgG. N=3 per group.

8) 7H why top 100 and top 10 TFs (text states top 7)? How was this determined? What are the "top 10 transcription factors"? How was it concluded that it must be STAT3 and not for example STAT1 which was labeled as enriched motif in 2L and S5L. Motif analysis usually cannot pin down the exact factor so both could be options.

Answer: We apologize for not clarifying this in the text. We will address each of your questions point-by-point below.

A) 7H why top 100 and top 10 TFs (text states top 7)? How was this determined? What are the "top 10 transcription factors"?

Answer: We sincerely apologize for the inadvertent error in the manuscript where "top 10" was mistakenly written as "top 7." Actually, the top 10 TFs were selected

from the old manuscript Figure 7I. In this figure, we utilized the Cistrome (http://dbtoolkit.cistrome.org/) public transcription factor database and predicted the top 20 transcription factors that might regulate IL-33 expression, we selected the top 10 transcription factors include SUMO2, JUN, STAT3, CHAT, EP300, CEBPD, CEBPB, FOS, BRD4, RELA, which have been presented in revised Figure 7 M. We are truly sorry for the missing description of the top 10 TFs. Here is the Cistrome Database-Based Screening Criteria:

1) Sorting metric: Transcriptional regulators were ranked by their regulatory potential score (RPS), a quantitative measure of predicted regulatory activity.

2) Selection threshold: The top 10 transcription factors (top 10) with the highest RPS values were prioritized.

3) Rationale: This approach ensures the inclusion of candidates demonstrating statistically significant regulatory effects on IL-33 expression.

Additionally, we performed motif enrichment analysis of differential peaks in ECs using scATAC-seq datasets of fibrotic mouse model and identified the top 100 motifs highly expressed in the endothelium (Figure 7N, Supplement table S13). Venn diagram analysis suggested that STAT3 is a key TF regulating IL-33 expression upon mechanical force (Figure 7N). Hereby we selected STAT3 as the downstream target of PIEZO1 to regulate IL-33.

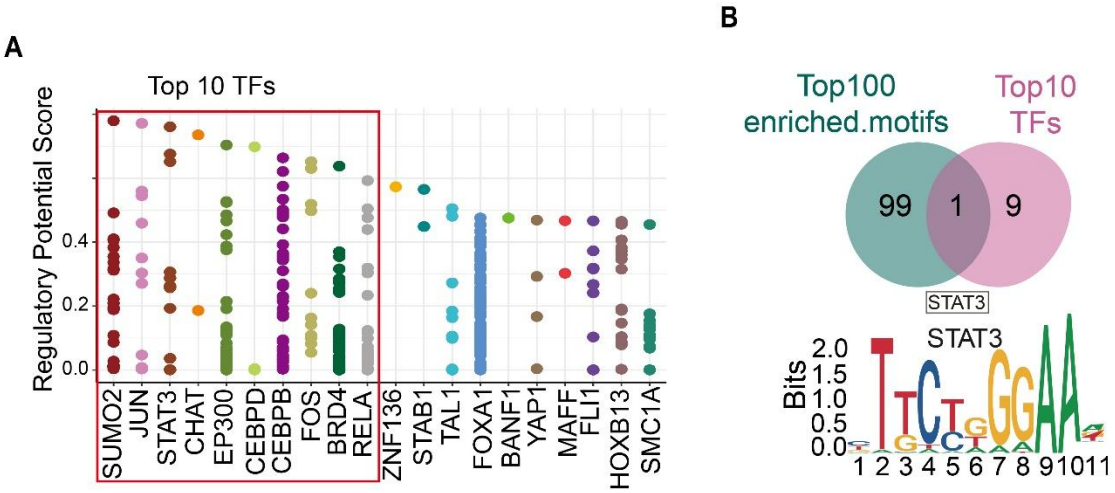

Figure to Reviewer 3: Screening process of the transcription factor STAT3 to regulate IL-33. (A) Cistrome database analysis predicts STAT3 as a key transcription factor in the regulation of IL-33 expression from Top 10 TFs. (B) Venn diagrams

indicating that the top 100 motifs in ECs of BLM-treated mice intersect with the top 10 transcription factors. **Data are shown in revised Figure.7M-N.**

B) How was it concluded that it must be STAT3 and not for example STAT1 which was labeled as enriched motif in 2L and S5L. Motif analysis usually cannot pin down the exact factor so both could be options.

Answer: We regret this oversight in our study. Our experiments revealed that both STAT3 and STAT1 were upregulated in cells exposed to mechanical tension or cultured on stiff substrates. However, PIEZO1 knockdown (via shPIEZO1) specifically suppressed STAT3 expression and phosphorylation, while STAT1 levels remained unaffected. These results suggest that mechanical regulation of STAT1 occurs through PIEZO1-independent pathways. Given this mechanistic distinction, we focused our subsequent investigations on STAT3.

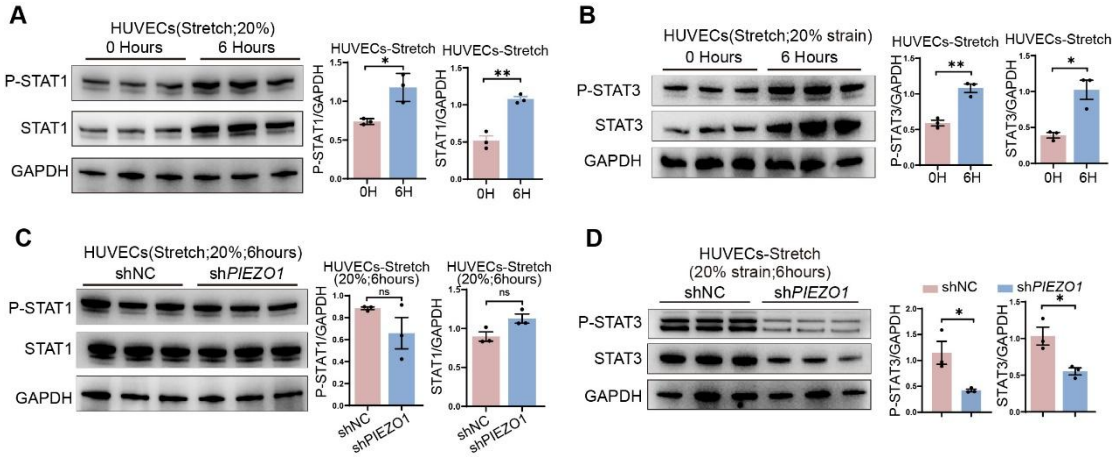

Figure to Reviewer 3: PIEZO1 can attenuate mechanical stretch-induced STAT3 phosphorylation, but not STAT1 phosphorylation. **B-D Data are shown in revised Fig.7O-P.; A-C are presented here exclusively.**

(A) The HUVECs treated with stretch (20%) for 0 and 6 hours. The protein levels of P-STAT1 and STAT1 in HUVECs were detected. N=3 per group.IgG. N=3 per group. (B) The HUVECs treated with stretch (20%) for 0 and 6 hours. The protein levels of P-STAT3 and STAT3 in HUVECs were detected. N=3 per group.(C) The protein levels of P-STAT1 and STAT1 in HUVECs were treated with stretch (20%) for 6 hours after transduced with sh*PIEZO1* for 48 hours. N=3 per group. (D) The protein levels of P-STAT3 and STAT3 in HUVECs were treated with stretch (20%) for 6 hours after transduced with sh*PIEZO1* for 48 hours. N=3 per group.

Minor:

1) From the writing it is unclear if the processing and annotation of scATAC-seq of Silica and BLM datasets (one mentions annotation based on prediction from scRNA and the latter looks at promoter accessibility). Please clarify.

Answer: We appreciate the reviewer's comment. Both scATAC-seq data of Silica and BLM data were annotated using scRNA-seq data of corresponding mouse model as references according to Seurat official guidance1. After identification of anchors between scRNA-seq and scATAC-seq data with FindTransferAnchors function using a CCA and MNNs, scRNA-seq and scATAC-seq data were integrated according to the anchors. Then the annotation of scRNA-seq data was projected onto the scATAC-seq data via the TransferData function.

Reference:

[1]. Stuart, Tim et al. “Comprehensive Integration of Single-Cell Data.” Cell, vol. 177,7 (2019): 1888-1902.e21. doi:10.1016/j.cell.2019.05.031

2) S4 panel legend F and G is switched. S5 description for panel I is incorrect.

Answer: We appreciate the reviewer’s comment. We have corrected the mistakes.

RE: Point-by-point response (NCOMMS-24-47968B)

Contents

Reviewer #1 (Remarks to the Author):

The authors have made extensive revisions to the manuscript in response to critiques from the reviewers. While several responses have addressed my prior comments and have improved the manuscript significantly, there are a number of issues that have not be adequately resolved and in places the revised results raise points that should be addressed.

1)The authors have removed textual assertions of increased endothelial cells in IPF lungs, although Figure 1D legend continues to state this. In the response letter, they support this assertion by citing three small scRNA-seq datasets. Because of issues related to cellular/nuclear disaggregation (particularly from fibrotic lungs), the assertion that sc/snRNA-seq more precisely quantifies cellular composition compared to histologic/tissue-based methods is not accurate. Specifically, relatively increased proportions of endothelial cells can be recovered when there is poor liberation or viability of alveolar epithelial cells and fibroblasts.

Answer: 1) We are sorry for the possible misunderstandings caused by our results. Here, we were trying to explain that the highest proportion of **Scissor+ cells (FVC-low phenotype (FLP) cells)** was found in endothelial cells (**Figure 1D of previous version**) **instead of the increase of endothelial cells in the lung tissues**. We adjusted the visualization of Figure 1D from the previous version to make it more accessible.

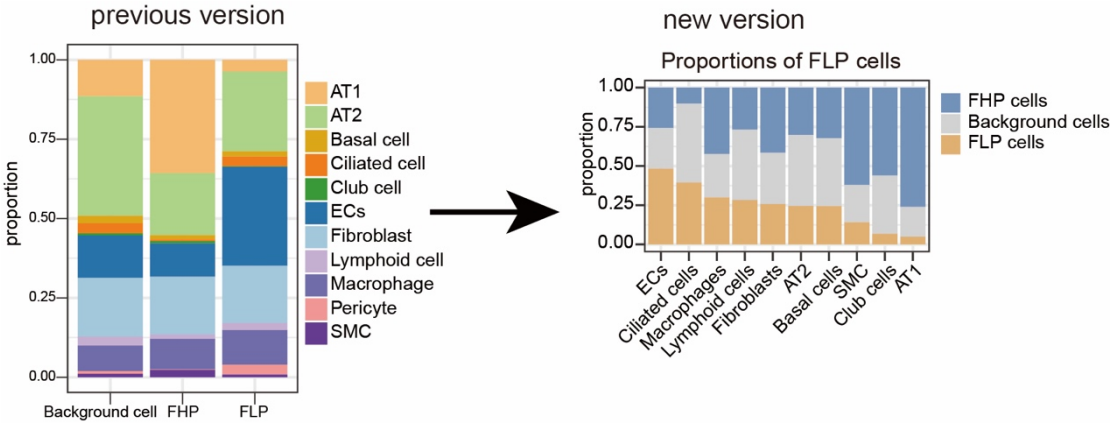

Figure1 to Reviewer 1: Change in display format of proportion of Scissor cell types.

2) We fully support your view that the numbers of endothelial cells are indeed not increased in fibrotic lungs. To further support your perspective, we analyzed public

datasets and classified the data according to different types of fibrotic lung disease. This analysis also confirmed that the total number of endothelial cells shows no significant change trend . Only venous endothelial cells were found to be upregulated. Thus, we contend that an exclusive focus on quantitative shifts in target cell populations during disease progression is inadequate, as such an approach risk neglecting functionally significant genes with critical ties to clinical markers. To bridge this gap, we introduce scissors single-cell analysis to systematically map relationships between clinical phenotypes and disease-associated cell subpopulations. Our analytical framework may further offer a methodological blueprint for future research in the field of respiratory diseases.

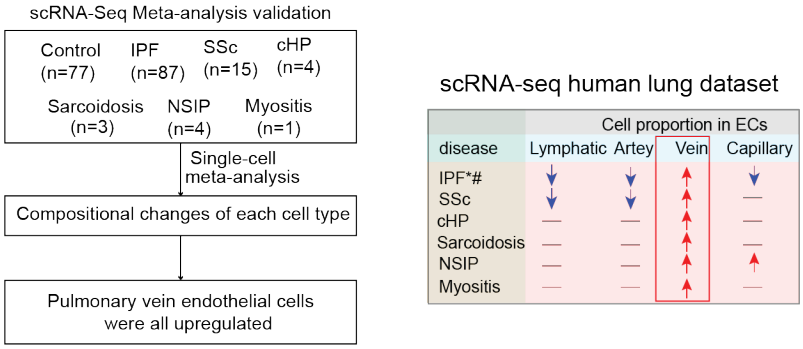

Figure2 to Reviewer 1: Schematic (Left)representation of the analysis of single-cell RNA sequencing data from lung tissues of patients with IPF and non-IPF-PF (chronic hypersensitivity pneumonitis (cHP), sarcoidosis, systemic sclerosis, myositis-ILD) in a multicenter public database, aiming to reveal new mechanisms and potential therapeutic targets of pulmonary fibrosis. Table (Right) shows a meta-analysis of the differences in the proportions of each endothelial cell subset (Lymphatic ECs, Artery ECs, Vein ECs, Capillary ECs)–in patients with different types of IPF and non-IPF-PF compared to healthy controls. scRNA-seq datasets: GSE122960, GSE128033, GSE128169, GSE132771, GSE135893, GSE136831 and GSE159354.

a. The plot from the Caporarello Nature Communications manuscript is plotting subpopulations of endothelial cells using total endothelial cells as the denominator – this is not quantifying endothelial cells in relation to total cells. Further, the cited reference for the primary date underlying that plot appears potentially incorrect – the reference refers to GSE136831 which included 32 IPF and 27 control lungs, yet only 3 dots per group are shown in this plot. Altogether, these results simply do not support the authors assertion that endothelial cells are increased in IPF lungs.

Answer: After carefully re-examining Caporarello et al.'s Nature Communications article, we concur with your perspective. The findings of Caporarello et al. indeed do

not support an increase in the total number of pulmonary endothelial cells in IPF patients.

b. The other referenced examples presented in the response letter (none of which report statistical differences in endothelial cells using appropriate methods including multiple testing correction), also suffer from the same "zero-sum" issue previously raised – if one population is reduced in scRNA-seq (for example, AT1 and AT2 cells), one must recover a larger proportion of other cell populations, even if absolute numbers are decreased – this is simply not a reliable method for compositional analyses.

Answer: We quite agree with you. The "zero-sum" issue is also presented in our analysis of new scRNA-seq data. Our analysis similarly revealed that scRNA-seq data from collected lung tissue samples showed greater abundance of immune cells, while parenchymal cells (including endothelial cells) were underrepresented.

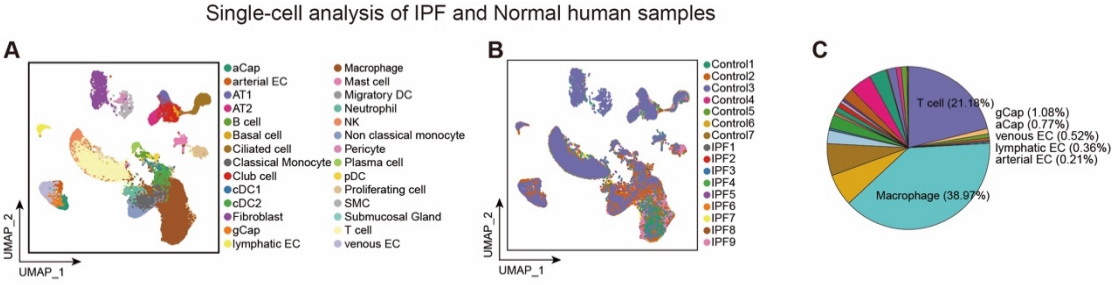

Figure3 to Reviewer 1: Analysis of newly collected scRNA-seq data from IPF and normal human samples revealed the "zero-sum" issue of scRNA-seq data.

c (1) Further, the largest IPF/ILD scRNA-seq datasets (GSE136831, GSE227136) show the opposite finding (while there are increased COL15A1+ systemic-venous type endothelial cells, dramatic reductions in capillary endothelial cells result in an overall decrease).

Answer: Upon re-analysis of scRNA-seq datasets (GSE122960, GSE128033, GSE128169, GSE132771, GSE135893, GSE136831, and GSE159354) stratified by IPF and non-IPF-PF categories-including chronic hypersensitivity pneumonitis (cHP), sarcoidosis, systemic sclerosis, and myositis-ILD-we consistently observed venous

endothelial upregulation and capillary downregulation in IPF group.

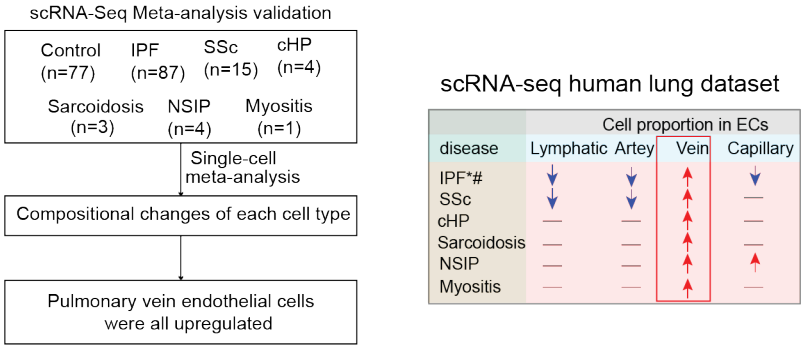

Figure4 to Reviewer 1: Schematic (Left) representation of the analysis of single-cell RNA sequencing data from lung tissues of patients with IPF and non-IPF-PF (chronic hypersensitivity pneumonitis (cHP), sarcoidosis, systemic sclerosis, myositis-ILD) in a multicenter public database, aiming to reveal new mechanisms and potential therapeutic targets of pulmonary fibrosis. Table (Right) shows a meta-analysis of the differences in the proportions of each endothelial cell subset (Lymphatic ECs, Artery ECs, Vein ECs, Capillary ECs) in patients with different types of IPF and non-IPF-PF compared to healthy controls. scRNA-seq datasets: GSE122960, GSE128033, GSE128169, GSE132771, GSE135893, GSE136831 and GSE159354.

c (2) In addition, three recent tissue-based spatial transcriptomic studies (PMID 38951642, 39121212, 39901013) also show, if anything, reduced endothelial cells – these methods, which are more accurate for compositional assessment than any disaggregation-based scRNA-seq method, should be considered much closer to a "gold standard."

Answer: To evaluate the proportion of endothelial cells more accurately, we reanalyzed the public Visium data (PMID: 39121212), and the result demonstrated that there is no significant change in endothelial cell proportion.

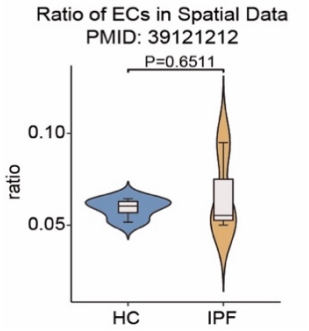

Figure5 to Reviewer 1: Proportions of ECs in HC and IPF groups of public data (PMID: 39121212).

As corroborating evidence, our spatial transcriptomic data from an independent specimen cohort (2 normal control and 2 IPF) confirmed unaltered endothelial cell frequencies .

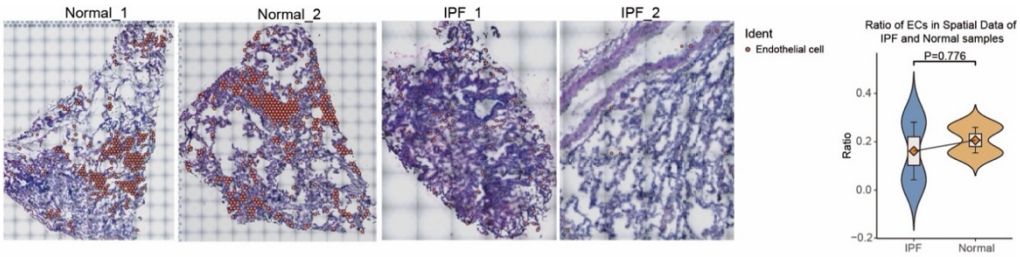

Figure 6 to Reviewer 1: Preliminary analysis of spatial transcriptomic sequencing data from our newly collected samples-including 2 idiopathic pulmonary fibrosis (IPF) and 2 normal controls revealed no statistically significant difference in endothelial cell abundance between IPF and normal groups.

d. The overall assertion of increased endothelial cells in IPF lungs is not ultimately very relevant to the authors proposed (and better supported) mechanistic studies, so I would recommend the compositional analyses and claims related to them be removed.

Answer: As you noted, we strongly agree with your point and have removed the compositional analyses from the manuscript.

2) The revised cell annotation appears much improved and more useful for readers to compare across publications and interpret these results.

Answer: We are deeply grateful for your constructive critique, which significantly strengthened our study.

3) The increased number of samples (now 4-5 per group) represents an improvement, though this is still a small dataset compared to the 100+ public IPF samples available

Answer: We are sorry for the inadequacy of snRNA-seq data. We had collected 9 IPF and 7 Control human samples for scRNA-seq and the same analytical process was performed. The results of scRNA-seq data are consistent with those of snRNA-seq data and GEO public data. However, the proportion of endothelial cells is low. **On account of "zero-sum" issue**, we did not choose to present the relevant results.

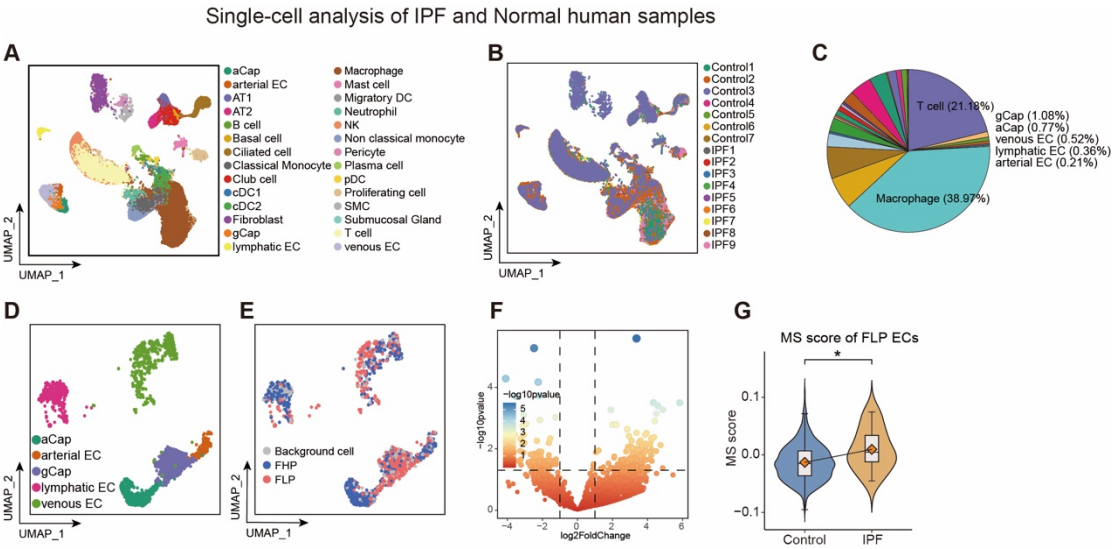

Figure7 to Reviewer 1: Reviewer 1: Analysis of new scRNA-seq data of IPF and Normal human samples.

4) The revised language clarifying that single-timepoint FVC reflects severity, not progression rate, is acceptable.

Answer: We are truly grateful for your suggestion and affirmation.

5) It is appreciated that the authors report the genes used for the "mechanical stress" score, but shouldn't the same set of genes be used for each of the analyses? It isn't clear why a different set of genes was used for human vs. house and was not consistent within human or within mouse experiments.

Answer: We quite agree with your comments. We unified the mechanical stress gene set of scoring for both human and mouse samples. Here, all the scoring for both human data and mouse data is corrected and based on the unified gene set "response to mechanical stress stimulus" obtained through enrichment analysis based on DEG analysis of pseudobulk-snRNA-data. The MS scoring was performed on human snRNA-seq data (**Figure 1H-I**), GEO public data (**Figure 1L-M, Supplementary Figure 2C**), Silica-induced mouse data (**Figure 2G-L**).

6)The revised fibrosis measures are improved, although in some experiments (Figure 4H-K, non-bleomycin treated controls are not reported.

Answer: We appreciate your advice and followed your important suggestions and repeated the experiments with the saline control group that was not treated with bleomycin, as well as the Yoda1 and GsmTx4 control groups.

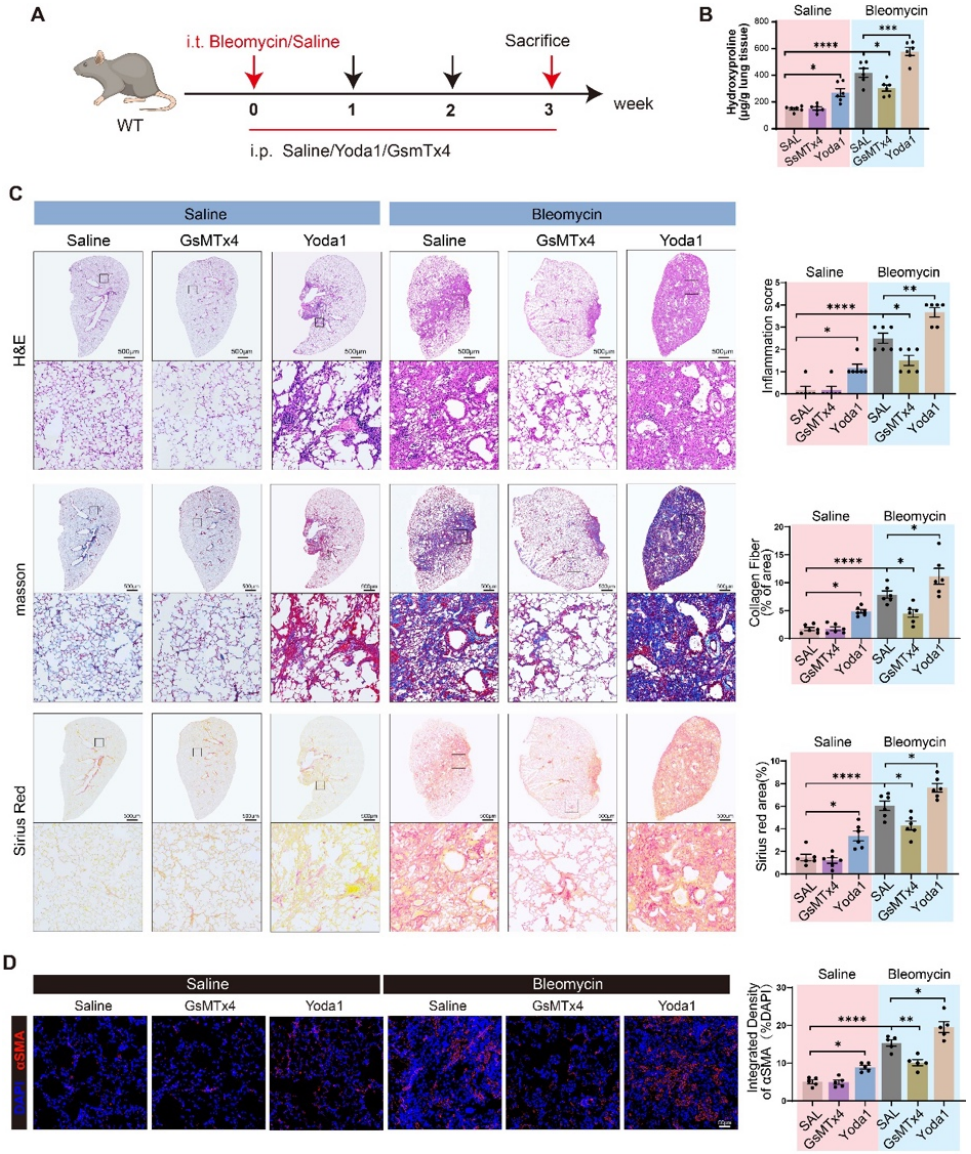

Figure8 to Reviewer 1: YODA1 and Gsmtx4 affect the fibrotic response in the mouse lung fibrosis model induced by bleomycin and saline control. **Data are shown in revised Figure 4H-I and Supplementary Figure 5G-H.**

(A) The schematic illustrates the treatment of BLM-induced pulmonary fibrosis with the *PIEZO1* agonist Yoda1 and the antagonist GsMTx4. Mice were euthanized after 3 weeks. (B)

The plot shows the hydroxyproline content in lung tissues from mice in the bleomycin- and saline-induced lung fibrosis model treated with Yoda1 or GsMTx4 via intraperitoneal injection (n = 6). (C) Representative images of H&E, Masson and Sirius red staining in fibrotic lungs of mice in Yoda1 or GsMTx4-induced via intraperitoneal. Quantification is shown at right (n = 6). (D) Immunofluorescent staining of αSMA (red) in fibrotic lungs of mice in Yoda1 or GsMTx4-induced via intraperitoneal. Representative co-staining image of indicated mouse lungs is shown, and quantification (percentage of αSMA $^{+}$ integrated density relative to DAPI $^{+}$) is shown at right (n = 6). Error bars represent mean ± SEM. Statistical significance was tested by one-way one-way ANOVA followed by Tukey's multiple comparisons test. *P < 0.05, **P < 0.01, ***P < 0.001 and ****P < 0.0001.

7)Revised Figure 1G: this still appears to be plotting differentially expressed genes across the entire endothelial cell group, which will reflect compositional differences. Subject-level, cell-type specific pseudobulk differential expression would be the rigorous and robust means of testing for differentially expressed genes among IPF subjects.

Answer: Thank you for your constructive advice. Pseudobulk analysis is indeed a better choice for DEGs under the circumstances. We have reanalyzed the data based on your comments, including DEG analysis of EC (**Figure 1G)** and EC subtypes.

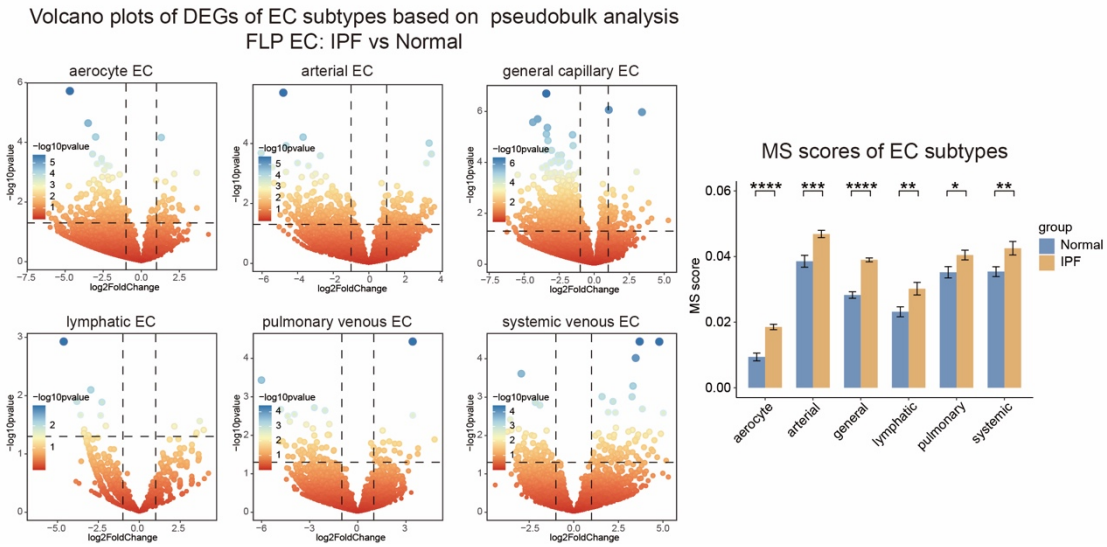

Figure 9 to Reviewer 1: Pseudobulk DEG analysis of FLP ECs (IPF vs Normal) and FLP EC subtypes (IPF vs Normal) and MS scores of EC and EC subtypes of IPF and Normal groups.

8)In line with comments from Reviewer 3, the Yoda-studies lack specificity; to have high confidence that these studies are mediating their effects through endothelial

Piezo 1, it would be necessary to test whether Yoda-treatment of endothelial Piezo1-deficient animals did or did not augment fibrosis.

Answer: We are grateful for your suggestions. Following your important advice, we intraperitoneally administered BLM-induced pulmonary fibrosis in *Piezo1* endothelial knockout mice treated with Yoda1 and analyzed the fibrotic response.

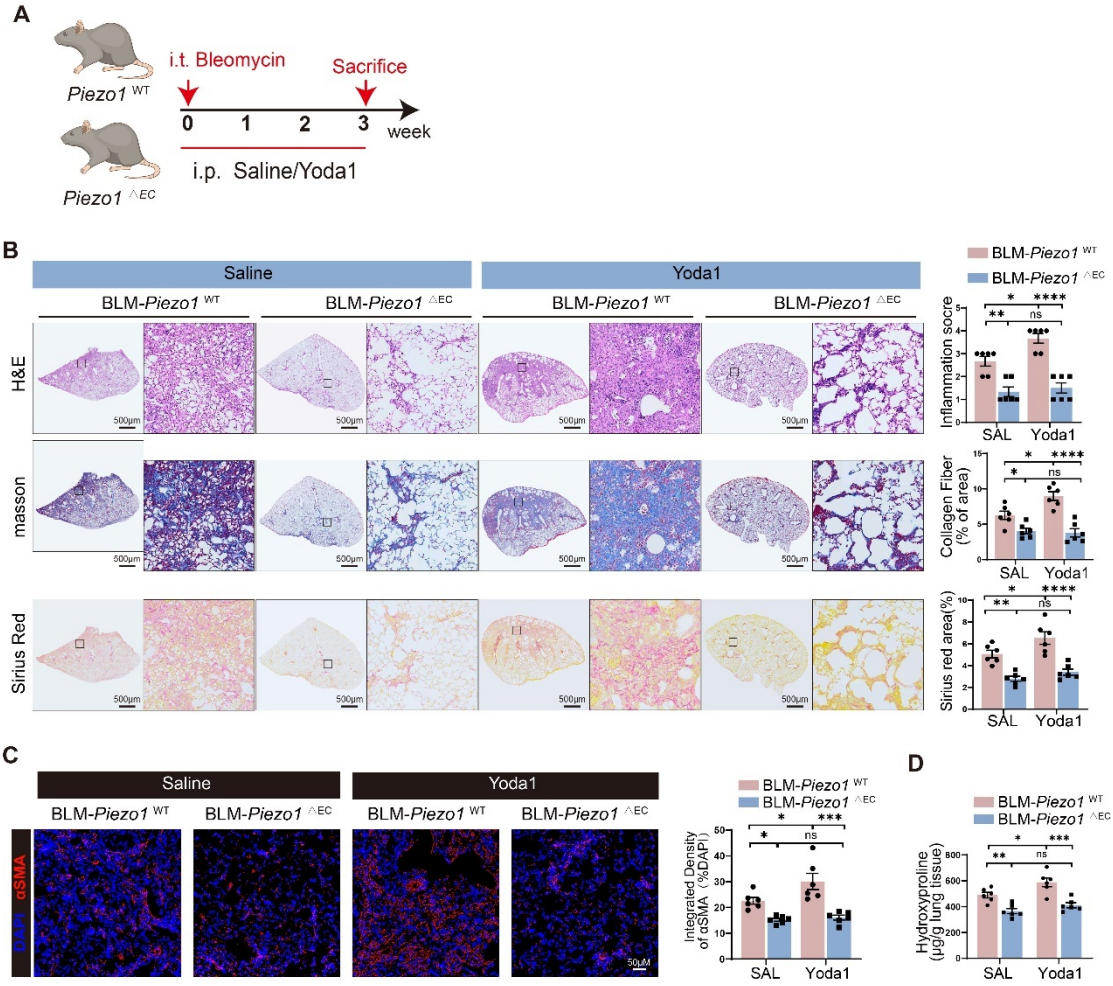

Figure10 to Reviewer 1: Yoda1 does not exacerbate BLM-induced pulmonary fibrosis in *Piezo1*$^{\Delta EC}$ mice. **Data are shown in revised Supplement Figure 6A-D.**

(A) The schematic illustrates intraperitoneal injection of Yoda1 for 3 weeks in BLM-induced pulmonary fibrosis models in *Piezo1*^{WT} and *Piezo1*$^{\Delta EC}$ mice. (B) Representative images of H&E, Masson and Sirius red staining in BLM-induced pulmonary fibrosis models in *Piezo1*^{WT} and *Piezo1*$^{\Delta EC}$ mice with Yoda1 and Saline. Quantification is shown at right (n = 6). (C) Immunofluorescent staining of αSMA (red) in BLM-induced pulmonary fibrosis models in *Piezo1*^{WT} and *Piezo1*$^{\Delta EC}$ mice with Yoda1 and Saline. Representative co-staining image of

indicated mouse lungs is shown, and quantification (percentage of αSMA $^{+}$ integrated density relative to DAPI $^{+}$) is shown at right (n = 6). (D) The plot shows the hydroxyproline content in lung tissues from mice in the bleomycin- and saline-induced lung fibrosis model treated with Yoda1 or GsMTx4 via intraperitoneal injection (n = 6). Error bars represent mean ± SEM. Statistical significance was tested by Two-way ANOVA followed by Tukey's multiple comparisons test. *P < 0.05, **P < 0.01, ***P < 0.001 and ****P < 0.0001.

9)The revised calpain studies add some strength to the overall body of evidence.

Answer: Thank you for recognizing the revised calpain studies.

10) In several panels where there are many groups in bar-plots(for example, figures 4 and 6), the statistical methods need to be included in the figure legends - it is difficult to assess these lacking details as to multiple testing adjustments, etc.

Answer: We appreciate your suggestion and will detail the statistical methods used in the experiments in the figure legends.

Minor comments:

1)For many figure legends, there is a space missing between Figure and the number.

Answer: Thank you for your suggestion. We have carefully proofread the figure legends in the manuscript.

2)In numerous places, the revised figure legends are interpretative of the results rather than descriptive of the study – the legends should describe the experiment, and any interpretation belongs in the main text (1D, 1H-I, 1O, 2I-J, 2L, 5G, 5I, others).

Answer: We truly appreciate your suggestion and the non-standard legends have been corrected.

Reviewer #2 (Remarks to the Author):

The authors have addressed all my comments fully.

Reviewer #3 (Remarks to the Author):

The authors have satisfactorily addressed most comments in the revision.

The regulation of IL33 locus by STAT-3 is not yet convincing. The authors acknowledge that YODA1 might not be the ideal system and have performed CUT&Tag-qPCR with 0h and 6h stretch. Why not replace the YODA1 data (Fig S7) with genome wide data using 0h and 6h stretch? In addition, a genome browser track of the location of the regions selected for CUT&Tag-qPCR would be very helpful. Finally, I am wondering how qPCR could show regulation if in the sequencing data there is no signal e.g. at the promoter.

Answer: We sincerely appreciate the reviewer's valuable suggestions. Considering that CUT&RUN is more advantageous than CUT&Tag for detecting transcription factor binding across the genome, we performed CUT&RUN experiments with both 0h and 6h stretching conditions, including IgG negative controls and H3K4me3 positive controls. Our results demonstrate that STAT3 binds to multiple sites in the upstream regulatory region of IL-33, covering the enhancer, promoter, as well as Peak1 and Peak2 regions that we previously identified.

While we acknowledge that the overall quality of our CUT&RUN data could be further improved, it still represents a significant advancement over our initial CUT&Tag results. Importantly, the binding pattern of STAT3 shows reasonable consistency with the H3K4me3 signal in these regions.

Regarding the reviewer's question about the discrepancy between CUT&Tag sequencing and qPCR results, we believe this is likely due to the relatively low abundance of STAT3-bound DNA. While such low-abundance binding might lead to significant bias during high-cycle amplification in library preparation for sequencing, qPCR with specific primers can still reliably detect these interactions due to its higher sensitivity for targeted amplification.

Furthermore, given the rapid activation kinetics of mechanotransduction signaling, we employed CUT&Tag-qPCR to assess the direct binding of STAT3 at the upstream regulatory region of the IL-33 gene following 3 hours of mechanical stretch. As showed in Figure , STAT3 binding showed significant enrichment at Peak1, Peak2, Enhancer1, and Enhancer2, with a similar increasing trend observed in the promoter region following activation of mechanosensitive pathways by stretch stimuli (20% for 3 hr).

We hope these additional experiments and explanations help address the reviewer's concerns about STAT3 regulation of the IL-33 locus.

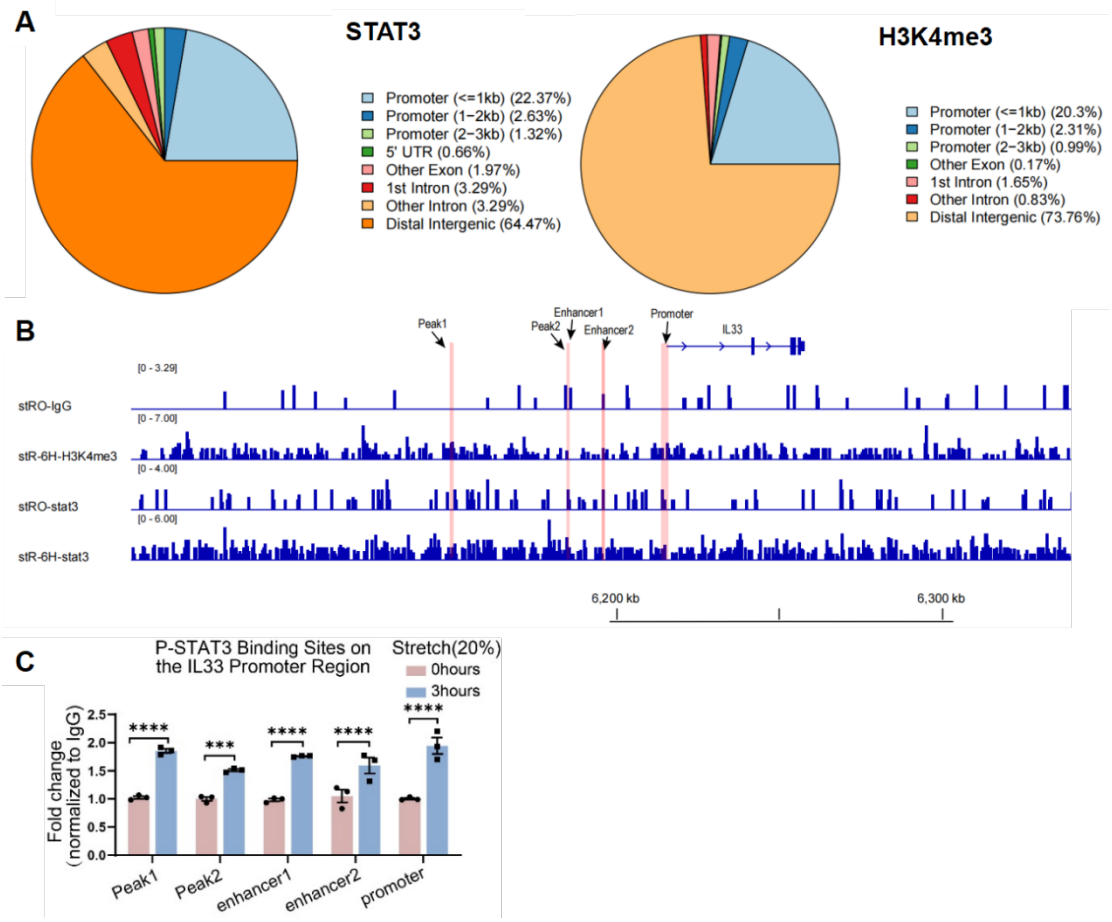

Figure1 to Reviewer 3:

(A) STAT3 and H3K4me3 peaks are broadly distributed across the genome of HUVEC after 6h stretch, including promoter regions, introns, and distal intergenic regions analyzed by CUT&RUN. (B) CUT&RUN was performed using a STAT3 antibody to identify binding sites of STAT3. The figure shows the sequencing results, highlighting the enrichment of STAT3 at specific genomic regions of IL-33. (C) Fold enrichment of P-STAT3 binding to the promoter region in HUVECs, as determined by Cut&Tag-qPCR. HUVECs were subjected to 20% stretch for 3 hours. Data are presented as fold enrichment relative to unstretched controls, normalized to IgG (n = 3).

RE: Point-by-point response (NCOMMS-24-47968B)

Contents

Reviewer #1 (Remarks to the Author):

The authors have made commendable efforts to address the issues raised in my prior comments and from the other reviewers. These changes have addressed my concerns satisfactorily.

Reviewer #3 (Remarks to the Author):

I appreciate the authors efforts to strengthen the data linked to direct regulation of IL33 by STAT-3.

I agree with the authors that CUT&RUN is better suited than CUT&Tag to profile transcription factor binding due to potential tagmentation of open chromatin by pA-Tn5.

Unfortunately, as also stated by the authors, the presented quality of CUT&RUN data in the revision is not high, e.g. the promoter mark H3K4me3 does not show the expected enrichment at promoter regions and distal peaks (e.g. peak 1) would be characterized by absence of H3K4me3 (Reviewer Figure 1A, B). The STAT3 signal does not appear different between peak and non-peak regions. Higher signal at peaks regions in 7S could also be explained by overall stronger signal across the whole locus as shown in Reviewer Figure 1B. Based on this it is very difficult to draw any robust conclusions of STAT3 binding from the analysis of the presented data.

Related to the CUT&Tag data: The explanation that the lack of signal at the IL33 promoter is due to a bias in library amplification is not convincing. For me it rather raises the question about what is amplified in qPCR? The signal in S7c overall is very sparse and comparing the peak calls with the signal tracks does not match well. I acknowledge that these experiments are difficult for TF and even more challenging for p-TFs.

Because of this, the presented data do not convincingly show direct regulation of IL33 by STAT. Thus, I think all what could be concluded is that STAT might directly control IL33.

Answer: Thanks for your careful review and valuable comments. We acknowledge and appreciate your concerns regarding the quality of the CUT&RUN and CUT&Tag data. Given the current limitations of the data, we have revised the manuscript (including the Abstract, Results, and Discussion sections) to ensure our claims are rigorous. Instead of asserting “direct regulation”, we now state that STAT3 “may directly regulate” or “is involved in the regulation of” IL33. We are grateful for your guidance and suggestions.